Open access • Journal Article • DOI:10.1002/NUM.20107

Anisotropic a posteriori error estimation for the mixed discontinuous Galerkin approximation of the Stokes problem — Source link

Emmanuel Creusé, Serge Nicaise

Institutions: University of Valenciennes and Hainaut-Cambresis

Published on: 01 Mar 2006 - Numerical Methods for Partial Differential Equations (Wiley Subscription Services, Inc., A Wiley Company)

Topics: Round-off error, Approximation error, Discontinuous Galerkin method, Estimator and Finite element method

Anisotropic a posteriori error estimation for the mixed discontinuous Galerkin approximation of the Stokes problem

Emmanuel Creusé, Serge Nicaise

Anisotropic a posteriori error estimation for the mixed discontinuous Galerkin approximation of the Stokes problem

Emmanuel Creusé   Serge Nicaise

Université de Valenciennes et du Hainaut-Cambrésis
MACS
Institut des Sciences et Techniques de Valenciennes
F-59313 - Valenciennes Cedex 9 France
Emmanuel.Creuse@univ-valenciennes.fr, Serge.Nicaise@univ-valenciennes.fr

Received

The paper presents a posteriori error estimates for the mixed discontinuous Galerkin approximation of the stationary Stokes problem. We consider anisotropic finite element discretizations, i.e. elements with very large aspect ratio. Our analysis covers two- and three-dimensional domains. Lower and upper error bounds are proved with minimal assumptions on the meshes. The lower error bound is uniform with respect to the mesh anisotropy. The upper error bound depends on a proper alignment of the anisotropy of the mesh which is a common feature of anisotropic error estimation. In the special case of isotropic meshes, the results simplify, and upper and lower error bounds hold unconditionally. The numerical experiments confirm the theoretical predictions and show the usefulness of the anisotropic error estimator.

Keywords: DG method, Error estimator, Anisotropic solution, Stretched elements, Stokes problem.

I. INTRODUCTION

In this paper we consider the stationary Stokes problem with Dirichlet boundary conditions in a bounded domain of the plane or of the space. In certain situations the solution has strong directional features, like edge singularities or boundary/interior layers.

When problems with anisotropic solutions are to be discretized, isotropic meshes are inappropriate, or they may even fail to give satisfactory results [1], indeed they would require very small element sizes in regions where the solution is anisotropic. Exemplarily we mention boundary layers where the finite elements have to be smaller than the layer width. Consequently this implies an extreme over-refinement in the layer. In order to avoid this drawback, a discretization has to be used which reflects the anisotropy.

Shishkin (type) meshes were one of the first discretizations to achieve this, see e.g. [1, 2]; geometric layer meshes are more recent ones [3, 4, 5]. Generally speaking, so-called anisotropic meshes are appropriate. They consist of elements where the aspect ratio can be very large, i.e. the ratio of the radii of the circumscribed and inscribed sphere is (potentially) unbounded. Although this is in contrast with the conventional, isotropic theory, the use of anisotropic discretizations allows to achieve the same accuracy with (much) less degrees of freedom. In our days, anisotropic elements can be applied favourably and are frequently applied. The theoretical aspects of anisotropic discretizations is now well understood [2, 6, 7, 8] and much efforts are undertaken to incorporate anisotropy into fully adaptive techniques.

Recently, discontinuous Galerkin methods have beeen developed for the approximation of different boundary value problems, like diffusion problems, see [9, 10] and the reference cited there, or the Stokes, Navier-Stokes problems [11, 12, 13, 14, 15]. In comparison with standard conforming methods the discontinuous Galerkin methods have several advantages, like robustness and stability in transport-dominated regimes, and flexibility in the mesh design.

Here we are concerned with a posteriori error estimators which are vitally important for adaptive algorithms and quality control. Particular emphasis is given to the Stokes problem in 3D domains since anisotropic solutions arise there generically.

For the Stokes problem, a posteriori error analyses of standard methods are available for isotropic discretizations [16, 17, 18, 19, 20, 21], as well as anisotropic ones [22, 23]. For discontinuous Galerkin methods, a posteriori analysis starts recently. For diffusion problems, residual error estimates are considered in [24, 25, 26], upper and lower error bounds being proved. For the 2D Stokes problem, an upper error estimate of residual type is proved in [27]. In these papers, the authors use isotropic meshes and therefore the energy-norm as well as the estimator are defined using isotropic quantities like the diameter of the elements. Therefore our goal is to extend the residual error estimator methods to anisotropic meshes in general 2D and 3D domains. The main point is to define an appropriate energy norm in order to obtain an (anisotropic) approximation property proved in [26] for isotropic meshes and extended here to anisotropic ones. Note that we will show that this property is optimal. With this property, defining appropriately the estimator we can prove an upper error bound, as well as a lower error bound. In other words, the proposed estimator is reliable and efficient. These results are furthermore confirmed by numerical experiments, that show that the error estimator is asymptotically equivalent to the error even for highly anisotropic meshes.

The paper is organized as follows. Section II. introduces the problem and some notation. The discretization and the discontinuous Galerkin method are given in Section III.. There minimal conditions on the mesh are presented and existence and uniqueness results are proved. Section IV. is devoted to analytical tools. We first recall the non-consistent reformulation of the DG method. We secondly prove the anisotropic approximation property using an appropriate energy norm and show its optimality. Since nonconforming meshes are allowed, we introduce adapted edge/face bubble functions and prove some inverse inequalities. Some specific anisotropic interpolation estimates are finally recalled. The error bounds are proved in Section V.. While all considerations are made for anisotropic meshes, we simplify the results for the case of an isotropic discretization in Section D. since even in that case we obtain new results (especially in 3D). The numerical experiments of Section VI. confirm our theoretical predictions.

II. PRELIMINARIES AND NOTATION

Let us fix a bounded domain Ω of $\mathbb{R}^d$, $d = 2$ or 3, with a Lipschitz boundary. On this domain we consider the Stokes problem

$$\left.\begin{aligned} -\nu\Delta u + \nabla p &= f && \text{in } \Omega \\ \operatorname{div} u &= 0 && \text{in } \Omega \\ u &= 0 && \text{on } \partial\Omega. \end{aligned}\right\} \tag{2.1}$$

To obtain its weak formulation, we introduce the spaces

$$\begin{aligned} V = H_0^1(\Omega)^d &:= \{v \in H^1(\Omega)^d : v = 0 \text{ on } \partial\Omega\}, \\ Q = L_0^2(\Omega) &:= \{q \in L^2(\Omega) : \int_\Omega q = 0\}, \end{aligned}$$

and the bilinear forms

$$a(u, v) := \nu \int_\Omega \nabla u : \nabla v, \qquad b(v, q) := -\int_\Omega q \operatorname{div} v,$$

where $\nu > 0$ is the viscosity of the fluid, ∇u means the matrix $(\partial_j u_i)_{1\leq i,j\leq d}$ (i being the index of row and j the index of column) and $\operatorname{div} u = \sum_{i=1}^d \partial_i u_i$ is the divergence of u. We further use the standard notation for the contraction of two matrices A and B, i.e.,

$$A : B := \sum_{i,j=1}^d A_{ij} B_{ij}.$$

According to Theorem I.5.1 of [28], for $f \in L^2(\Omega)^d$, there exists a unique solution $(u, p) \in V \times Q$ of

$$\left.\begin{aligned} a(u, v) + b(v, p) &= (f, v) \quad \forall v \in V, \\ b(u, q) &= 0 \qquad\;\; \forall q \in Q, \end{aligned}\right\} \tag{2.2}$$

where $(\cdot, \cdot)$ means the inner product in $[L^2(\Omega)]^d$ or in $L^2(\Omega)$ according to the context.

We end this section with some notation that will be used in the remainder of the paper: For two vectors $v, w \in \mathbb{R}^d$, we denote by $v \otimes w$ the matrix whose ij-th entry is $v_i w_j$.

If D is an open subset of Ω, the $L^2(D)$-norm is denoted by $\|\cdot\|_D$. In the case $D = \Omega$, we will drop the index Ω. Furthermore for $v \in L^2(\Omega)$, we set

$$\mathcal{M}_D v = \frac{1}{|D|} \int_D v,$$

where $|D|$ is the measure of D.

$\mathbb{P}^k$ and $\mathbb{Q}^k$ are the space of polynomials of total and partial degree not larger than k, respectively.

In order to avoid excessive use of constants, the abbreviations $x \lesssim y$ and $x \sim y$ stand for $x \leq cy$ and $c_1 x \leq y \leq c_2 x$, respectively, with positive constants c, c_1 and c_2 independent of x, y, the triangulation T_h and the viscosity parameter ν.

III. ANISOTROPIC DISCRETIZATION

The first two sections introduce general aspects of the discretization, e.g. the DG approximation. Section C. is then devoted to the introduction of *anisotropic quantities*. The general mesh assumptions are discussed afterwards in Section D.. As it turns out, the assumptions on the mesh which are introduced for anisotropic elements are quite weak, are standard in anisotropic a posteriori error analysis [6, 29, 30, 31, 32] and are similar to the ones for isotropic elements [26, 33, 27].

A. Discretization of the domain Ω

The domain Ω is discretized by a (possibly nonconforming) mesh T_h. In 2D, all elements are either triangles or rectangles. In 3D the mesh consists either of tetrahedra or of rectangular hexahedra, cf. also the figures of Section C.. The restriction to rectangle or rectangular hexahedra is only made for the sake of simplicity; the extension to parallelogram or hexahedra is straightforward.

Since we allow nonconforming meshes, in 2D, we suppose that the intersection between neighbouring elements is either a vertex or an edge of at least one of the two elements, while in 3D we suppose that the intersection between neighbouring elements is either a vertex or an edge or a face of at least one of the two elements.

Elements will be denoted by T, T_i or T', its edges (in 2D) or faces (in 3D) are denoted by E, while its vertices will be denoted by x. If the mesh is conforming the set of all (interior and boundary) edges (2D) or faces (3D) of the triangulation will be denoted by $\mathcal{E}$. If the mesh is nonconforming, then the set $\mathcal{E}$ is the set of edges/faces of smaller size, in other words, if $T \cap T'$ is not a full edge/face of T but an edge/face of T', then the edge/face of T is subdivided by the edges/faces of the neighbouring elements of T. The measure of an element or edge/face is denoted by $|T| := \mathrm{meas}_d(T)$ and $|E| := \mathrm{meas}_{d-1}(E)$, respectively. For each element $T \in T_h$, denote by n_T the unit outward normal vector along ∂T.

For our further analysis we need to define some jumps and means through any $E \in \mathcal{E}$ of the triangulation. For $E \in \mathcal{E}$ such that $E \subset \Omega$, denote by T^+ and T^- the two elements of T_h containing E. Let q, v, τ be scalar-, vector- and matrix-valued functions, respectively, defined on $T^+ \cup T^-$, and which are in H^1 inside each element $T^\pm$. We denote by $q^\pm$, $v^\pm$, $\tau^\pm$, the traces of q, v, τ on E taken from $T^\pm$, respectively. Then we define the mean of q, v, τ on E by

$$\{\{q\}\} = \frac{q^+ + q^-}{2}, \{\{v\}\} = \frac{v^+ + v^-}{2}, \{\{\tau\}\} = \frac{\tau^+ + \tau^-}{2}.$$

The different jumps on E are now defined as follows:

$$\begin{aligned} [\![q]\!] &= q^+ n_{T^+} + q^- n_{T^-}, \\ [\![v]\!] &= v^+ \cdot n_{T^+} + v^- \cdot n_{T^-}, \\ \underline{[\![v]\!]} &= v^+ \otimes n_{T^+} + v^- \otimes n_{T^-}. \end{aligned}$$

Remark that $[\![q]\!]$ is the jump of q but is vector-valued, $[\![v]\!]$ is the jump of the normal component of v is scalar-valued, while $\underline{[\![v]\!]}$, the full jump of v, is matrix-valued.

For a boundary edge/face E, i. e., $E \subset \partial\Omega$, there exists a unique element $T^+ \in T_h$ such that $E \subset \partial T^+$. Therefore the mean and jumps are defined as before by taking $q^- = 0$, $v^- = 0$ and $\tau^- = 0$.

If we have $v \in [H^1(T)]^d$ for all T in T_h, then we define its broken gradient $\nabla_h v$ in Ω by :

$$(\nabla_h v)_{|T} = \nabla v_{|T}, \forall T \in T_h.$$

Furthermore one requires local subdomains (also known as patches). As usual, let ω_T be the union of all elements T' such that $T \cap T' \in \mathcal{E}$. Similarly for $E \in \mathcal{E}$, ω_E is the union of all elements containing E.

Later on we specify additional, mild mesh assumptions that are partially due to the anisotropic discretization.

B. The discontinuous Galerkin method

Following [14, 27], we consider the following discontinuous Galerkin approximation of the continuous Stokes problem: Given a mesh T_h and a polynomial degree $k \geq 1$, we consider the approximation spaces

$$\begin{aligned} V_h &= \{v \in L^2(\Omega)^d : v_{|T} \in (P_T^k)^d, \forall T \in T_h\}, \\ Q_h &= \{q \in L_0^2(\Omega) : q_{|T} \in (P_T^{k-1}), \forall T \in T_h\}, \end{aligned}$$

where the space P_T^k is defined as follows:

$$\begin{aligned} P_T^k &= \mathbb{P}^k(T) \quad \text{if } T \quad \text{is a triangle or a tetrahedron,} \\ P_T^k &= \mathbb{Q}^k(T) \quad \text{if } T \quad \text{is a rectangle or a hexahedron.} \end{aligned}$$

The space V_h is equipped with the norm

$$\|v\|_{1,h} := \left(\|\nabla_h v\|_\Omega^2 + \sum_{E \in \mathcal{E}} h_E^{-1} \|\underline{[\![v]\!]}\|_E^2 \right)^{1/2},$$

while Q_h is simply equipped with the $L^2(\Omega)$-norm.

With these notation, we define the bilinear forms $a_h(.,.)$ and $b_h(.,.)$ as follows:

$$\begin{aligned} a_h(u,v) &:= \nu \sum_{T \in T_h} \int_T \nabla u : \nabla v - \sum_{E \in \mathcal{E}} \int_E (\{\{\nu \nabla_h v\}\} : \underline{[\![u]\!]} + \{\{\nu \nabla_h u\}\} : \underline{[\![v]\!]}) \\ &+ \nu\gamma \sum_{E \in \mathcal{E}} h_E^{-1} \int_E \underline{[\![u]\!]} : \underline{[\![v]\!]}, \qquad \forall u, v \in V_h, \\ b_h(u,q) &:= -\sum_{T \in T_h} \int_T q \operatorname{div} u + \sum_{E \in \mathcal{E}} \int_E \{\{q\}\} [\![u]\!], \qquad \forall u \in V_h, q \in Q_h, \end{aligned}$$

where the positive parameter γ is chosen large enough to ensure coerciveness of the bilinear form a_h (see Lemma 3.2 below).

The discontinous Galerkin approximation of problem (2.2) reads now: Find $u_h \in V_h$, $p_h \in Q_h$, such that

$$\left. \begin{aligned} a_h(u_h, v_h) + b_h(v_h, p_h) &= (f, v_h) \quad \forall v_h \in V_h, \\ b_h(u_h, q_h) &= 0 \qquad\quad \forall q_h \in Q_h. \end{aligned} \right\} \tag{3.1}$$

For isotropic meshes T_h made of rectangles or hexahedra, the mixed problem (3.1) is well-defined since it satifies a uniform discrete inf-sup condition [34, 14]. We will prove in subsection E. the well-posedness of problem (3.1) for all families of meshes considered here. Note further that the uniform inf-sup condition is not necessary to prove our error bounds.

C. Anisotropic finite element domains T

In our exposition T can be a triangle or rectangle (2D case), or a tetrahedron, or a (rectangular) hexahedron (3D case).

Parts of the analysis require *reference elements* $\hat{T}$ that can be obtained from the actual element T via some affine linear transformation. The table below lists the reference elements for each case. Furthermore for an element T we define 2 or 3 *anisotropy vectors* $p_{i,T}, i = 1 \dots d$, that reflect the main anisotropy directions of that element. These anisotropy vectors are defined and visualized in the table below as well.

Element T	Reference	element $\hat{T}$	Anisotropy vectors $p_{i,T}$
Triangle 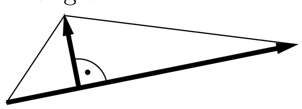	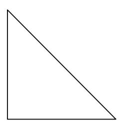	$0 \leq \hat{x}, \hat{y}$ $\hat{x} + \hat{y} \leq 1$	$p_{1,T}$ longest edge $p_{2,T}$ height vector
Rectangle 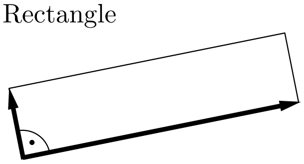	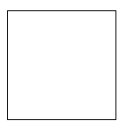	$0 \leq \hat{x}, \hat{y} \leq 1$	$p_{1,T}$ longest edge $p_{2,T}$ height vector
Tetrahedron 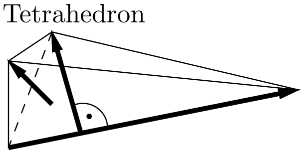	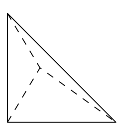	$0 \leq \hat{x}, \hat{y}, \hat{z}$ $\hat{x} + \hat{y} + \hat{z} \leq 1$	$p_{1,T}$ longest edge $p_{2,T}$ height in largest face that contains $p_{1,T}$ $p_{3,T}$ remaining height
Hexahedron 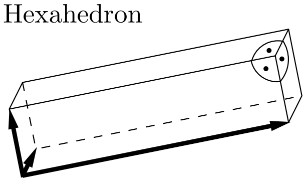	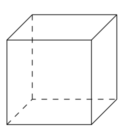	$0 \leq \hat{x}, \hat{y}, \hat{z} \leq 1$	$p_{1,T}$ longest edge $p_{2,T}$ height in largest face that contains $p_{1,T}$ $p_{3,T}$ remaining height

The anisotropy vectors $p_{i,T}$ are enumerated such that their lengths are decreasing, i.e. $|p_{1,T}| \geq |p_{2,T}| \geq |p_{3,T}|$ in the 3D case, and analogously in 2D. The *anisotropic lengths* of an element T are now defined by

$$h_{i,T} := |p_{i,T}|$$

which implies $h_{1,T} \geq h_{2,T} \geq h_{3,T}$ in 3D. The smallest of these lengths is particularly important; thus we introduce

$$h_{min,T} := h_{d,T} \equiv \min_{i=1\dots d} h_{i,T}.$$

Finally the anisotropy vectors $p_{i,T}$ are arranged columnwise to define a matrix

$$\left.\begin{array}{lll} C_T &:=& [p_{1,T}, p_{2,T}] \in \mathbb{R}^{2\times 2} \quad \text{in 2D} \\ C_T &:=& [p_{1,T}, p_{2,T}, p_{3,T}] \in \mathbb{R}^{3\times 3} \quad \text{in 3D.} \end{array}\right\} \tag{3.2}$$

Note that C_T is orthogonal since the anisotropy vectors $p_{i,T}$ are orthogonal too, and

$$C_T^\top C_T = \operatorname{diag}\{h_{1,T}^2, \ldots, h_{d,T}^2\}.$$

Furthermore introduce the *height* $h_{E,T}$ over an edge/face E of an element T by

$$h_{E,T} := \frac{|T|}{|E|} \cdot \begin{cases} 1 & T \text{ is rectangle or hexahedron} \\ d & T \text{ is triangle or tetrahedron.} \end{cases}$$

D. Requirements on the mesh

Let us first introduce the following notation: For an element T, $\mathcal{N}_T$ is the set of (Lagrange) nodes of P_T^k, namely if $\hat{T}$ is the reference triangle or tetrahedron, denote by $\hat{a}_i, i = 1, \cdots, d+1$ its set of vertices and $\hat{\lambda}_i$, the associated barycentric coordinates, then take

$$\begin{aligned} \mathcal{N}_{\hat{T}} \quad &= \{\hat{x} = \sum_{j=1}^{d+1} \hat{\lambda}_j \hat{a}_j : \sum_{j=1}^{d+1} \hat{\lambda}_j = 1, \\ &\hat{\lambda}_j \in \{0, \frac{1}{k}, \cdots, \frac{k-1}{k}, 1\}, 1 \leq j \leq d+1\}. \end{aligned}$$

Similarly if $\hat{T}$ is the reference square or cube, we set

$$\mathcal{N}_{\hat{T}} = \{\hat{x} = (\frac{i_1}{k}, \cdots, \frac{i_d}{k})^\top : i_j \in \{0, 1, \cdots, k\}, 1 \leq j \leq d\}.$$

For an element T, we take

$$\mathcal{N}_T = F_T(\mathcal{N}_{\hat{T}}),$$

where F_T is the affine transformation mapping $\hat{T}$ to T. Recall that the triple (T, P_T^k, Σ_T) is a Lagrange finite element with $\Sigma_T = \{p(n)\}_{n\in\mathcal{N}_T}$ [35]. Denote by $\{\lambda_x^T\}_{x\in\mathcal{N}_T}$ the associated basis of P_T^k.

Let us finally set $\mathcal{N} = \cup_{T\in T_h}\mathcal{N}_T$, the set of nodes of the triangulation T_h, and $\mathcal{N}(\Omega) = \mathcal{N} \cap \Omega$, the set of interior nodes.

If the mesh is nonconforming, we subdivide its elements into levels (compare with [26]): First we say that a node $n \in \mathcal{N}$ is a hanging node of the mesh if $n \in T \cap T'$ and if $n \in \mathcal{N}_T \setminus \mathcal{N}_{T'}$. The level zero corresponds to the elements T such that any hanging node n of the mesh such that $n \in T$ belongs to $\mathcal{N}_T$. The level one is the level zero of the triangulation obtained from T_h by removing the elements of level zero. The next levels are defined iteratively.

The mesh has to satisfy some mild assumptions, see [6, 22, 26]

- A vertex of the mesh is contained only in a bounded number of elements.
- The size of neighbouring elements does not change rapidly, i.e.

$$h_{i,T_1} \sim h_{i,T_2} \qquad \forall i = 1\ldots d, \forall T_1 \cap T_2 \neq \emptyset.$$

- Since the mesh may be nonconforming (i.e. hanging nodes may exist), we suppose that for any neighbouring elements T and T' such that $T \cap T'$ is an edge/face E' of T' but not of T, then we assume that the edge/face E of T such that $E' \subset E$ satisfies $|E| \lesssim |E'|$.
- If the mesh is nonconforming, the number of levels is supposed to be bounded.

Note that the third assumption is quite realistic, since standard subdivision rules like regular refinements or edge bisections [36] imply it, while it is satisfied by isotropic meshes considered in [26, 27] and by nonconforming geometric layer meshes used in [3, 4, 5].

Sometimes it is more convenient to have *edge/face related* data instead of *element related* data. Hence for $E \in \mathcal{E}$ such that $E \subset \Omega$ and $E \subset T_1 \cap T_2$ we introduce

$$h_{min,E} := \frac{h_{min,T_1} + h_{min,T_2}}{2} \qquad \text{and} \qquad h_E := \frac{h_{E,T_1} + h_{E,T_2}}{2}.$$

For boundary edges/faces $E \subset \partial T$ simply set $h_{min,E} := h_{min,T}$, $h_E := h_{E,T}$. The second mesh assumption readily implies

$$h_E \sim h_{E,T_1} \sim h_{E,T_2} \qquad \text{and} \qquad h_{min,E} \sim h_{min,T_1} \sim h_{min,T_2}.$$

Note that Lemma 3.1 of [30] shows that

$$h_{min,T} \lesssim h_{E,T}, \tag{3.3}$$

and by the above assumptions, we deduce that

$$h_{min,E} \lesssim h_E. \tag{3.4}$$

E. Existence and uniqueness results

As usual, the mixed problem (3.1) is well-posed if a_h is coercive and b_h satisfies a (discrete) inf-sup condition. We will now check both properties.

The coercivity of the bilinear form a_h is based on the following inverse inequality:

Lemma 3.1. *For all $T \in T_h$ and any edge/face E of T, it holds*

$$h_E \|q\|_E^2 \lesssim \|q\|_T^2, \forall q \in P_T^{k-1}. \tag{3.5}$$

Proof. By a scaling argument, we have :

$$\|q\|_E \sim |E|^{\frac{1}{2}} \|\hat{q}\|_{\hat{E}} \lesssim |E|^{\frac{1}{2}} (\|\hat{q}\|_{\hat{E}} + \|\hat{q}\|_{\hat{T}}).$$

Since $\| \cdot \|_{\hat{E}} + \| \cdot \|_{\hat{T}}$ is a norm on $P_{\hat{T}}^{k-1}$, and since all norms are equivalent in a finite-dimensional space, we have

$$\|q\|_E^2 \lesssim |E||T|^{-1} \|q\|_T^2,$$

again by a scaling argument. The conclusion directly follows from this estimate and the property $h_E \sim h_{E,T} \sim |E||T|^{-1}$, which is a consequence of the mesh assumptions. ∎

Lemma 3.2. *If $\gamma > 0$ is large enough, then the bilinear form a_h is coercive on V_h, in other words,*

$$a_h(v_h, v_h) \gtrsim \|v_h\|_{1,h}^2, \forall v_h \in V_h.$$

Proof. By the definition of a_h, we have

$$\begin{aligned} a_h(u,u) \;:=\; & \nu\|\nabla_h u\|^2 + \nu\gamma \sum_{E\in\mathcal{E}} h_E^{-1}\|\underline{[\![u]\!]}\|_E^2 \\ & -\; 2\sum_{E\in\mathcal{E}}\int_E \{\{\nu\nabla_h u\}\} : \underline{[\![u]\!]}. \end{aligned}$$

Therefore by Cauchy-Scwharz's inequality and Young's inequality ($2ab \le \frac{a^2}{\varepsilon} + \varepsilon b^2$, for any $\varepsilon > 0$ and any real numbers a, b), we get

$$\begin{aligned} a_h(u,u) \;\ge\; & \nu\|\nabla_h u\|^2 + \nu \sum_{E\in\mathcal{E}} (\gamma - \varepsilon^{-1}) h_E^{-1}\|\underline{[\![u]\!]}\|_E^2 \\ & -\; \nu\varepsilon \sum_{E\in\mathcal{E}} h_E \|\{\{\nabla_h u\}\}\|_E^2. \end{aligned}$$

By Lemma 3.1 and the mesh assumptions, we arrive at

$$a_h(u,u) \ge \nu\|\nabla_h u\|^2(1 - C_1\varepsilon) + \nu \sum_{E\in\mathcal{E}} (\gamma - \varepsilon^{-1}) h_E^{-1}\|\underline{[\![u]\!]}\|_E^2,$$

for some positive constant C_1 (independent of γ). The conclusion follows by chosing ε and γ such that $1 - C_1\varepsilon > 0$ and $\gamma - \varepsilon^{-1} > 0$. ■

We now pass to the well-posedness of problem (3.1).

Lemma 3.3. *If γ is large enough, problem (3.1) has a unique solution $(u_h, p_h) \in V_h \times Q_h$, for all $f \in L_0^2(\Omega)^d$.*

Proof. By the finite dimensional character of problem (3.1), it suffices to prove the uniqueness of a solution in the homogeneous case, i.e., when $f = 0$. In that case, taking first $v_h = u_h$ in the first identity of (3.1) and taking into account the second one, we get

$$a_h(u_h, u_h) = 0.$$

By the previous lemma, we deduce that $u_h = 0$. Consequently p_h satisfies

$$b_h(v_h, p_h) = 0, \forall v_h \in V_h. \tag{3.6}$$

In a first step, for all $T \in T_h$, we consider $u_T \in H_0^1(T)^d$ satisfying

$$\operatorname{div} u_T = p_h - \mathcal{M}_T p_h \text{ on } T,$$

whose existence follows from Corollary I.2.4 of [28]. Define v_h on each element T by

$$v_{h|T} = \Pi_T u_T,$$

where Π_T is the Fortin operator associated with the pair $(M_{k-1}(T), D_{k-1}(T))$, the finite dimensional spaces $M_k(T)$ and $D_k(T)$, where $k \in \mathbb{N}$, corresponding to the Raviart-Thomas elements described in the table below, see section III.3 of [37]:

Element	$M_k(T)$	$D_k(T)$
Triangle/Tetra	$RT_k := [\mathbb{P}^k]^d + x\widetilde{\mathbb{P}}^k$	$\mathbb{P}^k$
Rectangle	$\mathbb{P}^{k+1,k} \times \mathbb{P}^{k,k+1}$	$\mathbb{Q}^k$
Hexahedra	$\mathbb{P}^{k+1,k,k} \times \mathbb{P}^{k,k+1,k} \times \mathbb{P}^{k,k,k+1}$	$\mathbb{Q}^k$

Here $\widetilde{\mathbb{P}}^k$ means the space of homogeneous polynomials of degree k, $\mathbb{P}^{k+1,k}$ the space of polynomials of degree $k+1$ in x_1 and of degree k in x_2 and $\mathbb{P}^{k+1,k,k}$ the space of polynomials of degree $k+1$ in x_1 and of degree k in x_2 and x_3.

By the properties of this Fortin operator, v_h belongs to V_h and satisfies

$$\begin{aligned}
&\operatorname{div} v_h = p_h - \mathcal{M}_T p_h \text{ on } T, \forall T \in T_h,\\
&v_{h|T} \cdot n_T = 0 \text{ on } \partial T, \forall T \in T_h.
\end{aligned}$$

Consequently, for this v_h we have

$$b_h(v_h, p_h) = -\sum_{T\in T_h} \int_T p_h(p_h - \mathcal{M}_T p_h) = -\sum_{T\in T_h} \int_T (p_h - \mathcal{M}_T p_h)^2.$$

By (3.6), we then obtain that

$$p_h = \mathcal{M}_T p_h \text{ on } T, \forall T \in T_h,$$

in other words p_h is piecewise constant.

In a second step, we define

$$\Omega_h = \Omega \setminus \mathcal{E}_{hanging},$$

where $\mathcal{E}_{hanging}$ is the set of hanging edges/faces, namely

$$\mathcal{E}_{hanging} = \{E \in \mathcal{E} : \exists T_1, T_2 \in T_h : E = T_1 \cap T_2, E \text{ is not an edge/face of } T_1\}.$$

If Ω_h is connected, we consider the unique solution $z \in H^1(\Omega_h)/\mathbb{R}$ of

$$\begin{cases} \Delta z = p_h & \text{in } \Omega_h,\\ \frac{\partial z}{\partial n} = 0 & \text{on } \partial\Omega_h. \end{cases}$$

By Theorem 23.3 of [38], z belongs to $H^{3/2-\epsilon}(\Omega_h)$, for any $\epsilon > 0$ and consequently setting $v = \nabla z$, $v_h = \Pi_h^0 v$ is meaningful, belongs to V_h and satisfies

$$\begin{aligned}
&\operatorname{div} v_h = p_h \text{ on } T, \forall T \in T_h,\\
&v_{h|T} \cdot n_T = 0 \text{ on } E \in \mathcal{E}_{hanging}, E \subset T, \forall T \in T_h,\\
&v_{h|T} \cdot n_T = 0 \text{ on } E \in \mathcal{E} \cap \partial\Omega, E \subset T, \forall T \in T_h,\\
&[\![v_h]\!] = 0 \text{ on } E, \forall E \in \mathcal{E} \setminus \mathcal{E}_{hanging}.
\end{aligned}$$

Here above and below Π_h^0 means the Fortin operator associated with the pairs $(M_0(T), D_0(T))$.

These properties imply that

$$b_h(v_h, p_h) = -\sum_{T\in T_h} \int_T (p_h)^2, \tag{3.7}$$

and therefore $p_h = 0$.

If Ω_h is not connected, we write

$$\Omega_h = \cup_{i=1}^{I} \Omega_h^i,$$

where each Ω_h^i is connected. For each $i = 1, \cdots, I$, let $z^i \in H^1(\Omega_h^i)/\mathbb{R}$ be the unique solution of

$$\begin{cases} \Delta z^i = p_h - \mathcal{M}_{\Omega_h^i} p_h & \text{in } \Omega_h^i, \\ \frac{\partial z^i}{\partial n} = 0 & \text{on } \partial\Omega_h^i. \end{cases}$$

As before z^i belongs to $H^{3/2-\epsilon}(\Omega_h^i)$, for any $\epsilon > 0$, and consequently setting $v = \nabla z^i$ on each Ω_h^i, we may define $v_h = \Pi_h^0 v$, which belongs to V_h and satisfies

$$b_h(v_h, p_h) = -\sum_{i=1}^{I} \int_{\Omega_h^i} (p_h - \mathcal{M}_{\Omega_h^i} p_h)^2.$$

This yields

$$p_h = \mathcal{M}_{\Omega_h^i} p_h \text{ in } \Omega_h^i, \forall i = 1, \cdots, I,$$

or equivalently p_h is constant on each Ω_h^i.

To conclude we need to build another v_h in V_h and that satisfies (3.7). For that purpose, denote by $\mathcal{F}$, the set of the edges/faces E of any $T \in T_h$ such that $E \subset \partial\Omega_h^i \cap \partial\Omega_h^j$, for some $i \neq j$, $E \subset \Omega$ and $E \notin \mathcal{E}_{hanging}$. Any $E \in \mathcal{F}$ is a finite union of elements from $\mathcal{E}_{hanging}$, we then fix one $F_E \in \mathcal{E}_{hanging}$ such that $F_E \subset E$. We consider the domain

$$\tilde{\Omega}_h = \Omega_h \cup \{F_E : E \in \mathcal{F}\}.$$

Since $\int_{\tilde{\Omega}_h} p_h = \int_\Omega p_h = 0$ and $\tilde{\Omega}_h$ is connected, we may consider the unique solution $w \in H^1(\tilde{\Omega}_h)/\mathbb{R}$ of

$$\begin{cases} \Delta w = p_h & \text{in } \tilde{\Omega}_h, \\ \frac{\partial w}{\partial n} = 0 & \text{on } \partial\tilde{\Omega}_h. \end{cases}$$

As before we take $v_h = \Pi_h^0(\nabla w)$ which belongs to V_h. Let us show that

$$\sum_{E\in\mathcal{E}} \int_E \{\{p_h\}\} [\![v_h]\!] = 0. \tag{3.8}$$

Indeed by construction $[\![v_h]\!] = 0$ on any $E \in \mathcal{E} \setminus \mathcal{E}_{hanging}$; on the other hand, any $F \in \mathcal{E}_{hanging}$ is included into an edge/face E of $\mathcal{F}$, therefore the above sum reduces to

$$\sum_{E\in\mathcal{E}} \int_E \{\{p_h\}\} [\![v_h]\!] = \sum_{E\in\mathcal{F}} \sum_{F\in\mathcal{E}_{hanging}:F\subset E} \int_F \{\{p_h\}\} [\![v_h]\!].$$

Now for a fixed $E \in \mathcal{F}$, we denote by T the element in T_h such that E is an edge/face of T. Then by the definition of the sets Ω_h^i, the element T is included into a unique Ω_h^i, the other elements T' such that $E \cap T'$ belongs to $\mathcal{E}_{hanging}$ being included into a set Ω_h^j, with $j \neq i$. Consequently $\{\{p_h\}\} = m_E \in \mathbb{R}$ on the whole E and therefore

$$\sum_{E\in\mathcal{E}} \int_E \{\{p_h\}\} [\![v_h]\!] = \sum_{E\in\mathcal{F}} m_E \sum_{F\in\mathcal{E}_{hanging}:F\subset E} \int_F [\![v_h]\!].$$

This means that (3.8) holds if one can show that

$$\sum_{F\in\mathcal{E}_{hanging}:F\subset E}\int_F [\![v_h]\!] = 0,$$

for all edge/face $E \in \mathcal{F}$.

We now fix $E \in \mathcal{F}$ and use the above notation. The properties of Π_h^0 and the boundary condition satisfied by w imply that (recalling that any element of $F \in \mathcal{E}_{hanging}$ is a full edge/face of a unique element from T_h, that we write T_F)

$$\begin{aligned}
&\int_E v_{h|T}\cdot n_T = \int_E (\nabla w)\cdot n_T = \int_{F_E} (\nabla w)\cdot n_T,\\
&\int_F v_{h|T_F}\cdot n_{T_F} = \int_F (\nabla w)\cdot n_{T_F} = 0, \forall F \in \mathcal{E}_{hanging}, F\subset E, F\neq F_E,\\
&\int_{F_E} v_{h|T_{F_E}}\cdot n_{T_{F_E}} = \int_{F_E} (\nabla w)\cdot n_{T_{F_E}}.
\end{aligned}$$

These identities yield

$$\sum_{F\in\mathcal{E}_{hanging}:F\subset E}\int_F [\![v_h]\!] = \int_E v_{h|T}\cdot n_T - \sum_{F\in\mathcal{E}_{hanging}:F\subset E}\int_F v_{h|T_F}\cdot n_{T_F} = 0,$$

and lead to the requested identity.

The identity (3.8) and again the properties of Π_h^0 allow to conclude that (3.7) holds for the last element v_h. ∎

Note that we have proved the implication:

$$b_h(v_h, p_h) = 0, \forall v_h \in V_h \Rightarrow p_h = 0,$$

which is equivalent to the non uniform inf-sup condition:

$$\sup_{v_h\in V_h}\frac{b_h(v_h,q_h)}{\|v_h\|_{1,h}} \geq \beta_h\|q_h\|,$$

for some $\beta_h > 0$.

IV. ANALYTICAL TOOLS

Since we treat *anisotropic elements*, some analytical tools which are known from the standard theory have to be reinvestigated. This is mainly due to the fact that the aspect ratio of the elements is no longer bounded, as it is the case with isotropic elements.

We emphasize on an approximation result, some inverse inequality and to anisotropic interpolation error estimates. In that last case, the use of anisotropic elements leads to a so-called *alignment measure*, cf. below. It is important to notice that this alignment measure is not a (theoretical or practical) obstacle to efficient and reliable error estimation.

A. The perturbed formulation

Following [10, 39, 27], we introduce a non-consistent reformulation of the variational problem (3.1). For that purpose we define the space

$$V(h) = H_0^1(\Omega)^d + V_h,$$

equipped with the broken energy norm $\|v\|_{1,h}$. Let us further introduce the auxiliary (matrix-valued) space

$$\Sigma_h = \{\tau \in L^2(\Omega)^{d\times d} : \tau_{|T} \in (P_T^k)^{d\times d}, \forall T \in T_h\}.$$

At this stage we introduce the lifting operators $L : V(h) \to \Sigma_h$ and $M : V(h) \to Q_h$ as follows:

$$\begin{aligned} \int_\Omega L(v) : \tau \, dx &= \sum_{E\in\mathcal{E}} \int_E \underline{[\![v]\!]} : \{\{\tau\}\}, \forall \tau \in \Sigma_h, \\ \int_\Omega M(v) q \, dx &= \sum_{E\in\mathcal{E}} \int_E [\![v]\!] \, \{\{q\}\}, \forall q \in Q_h. \end{aligned}$$

The above lifting operators has the following stability properties (compare with [10, 39, 27]):

Lemma 4.1. *For all $v \in V(h)$ it holds*

$$\|L(v)\|^2 + \|M(v)\|^2 \lesssim \sum_{E\in\mathcal{E}} \int_E h_E^{-1} |\underline{[\![v]\!]}|^2.$$

Proof. For $v \in V_h$, take $\tau = L(v) \in \Sigma_h$, then by the definition of $L(v)$, we may write

$$\|L(v)\|^2 = \int_\Omega L(v) : \tau \, dx = \sum_{E\in\mathcal{E}} \int_E \underline{[\![v]\!]} : \{\{\tau\}\}.$$

By Cauchy-Schwarz's inequality we obtain

$$\|L(v)\|^2 \le \sum_{E\in\mathcal{E}} \|\underline{[\![v]\!]}\|_E \|\{\{\tau\}\}\|_E.$$

But a standard scaling argument and the fact that all norms are equivalent in a finite dimensional space yield

$$\|\{\{\tau\}\}\|_E \lesssim h_E^{-1/2} \sum_{T\subset\omega_E} \|\tau\|_T. \tag{4.1}$$

Inserting this estimate in the previous one leads to

$$\|L(v)\|^2 \lesssim \sum_{E\in\mathcal{E}} h_E^{-1/2} \|\underline{[\![v]\!]}\|_E \left(\sum_{T\subset\omega_E} \|\tau\|_T \right).$$

Using the discrete Cauchy-Schwarz's inequality we arrive at

$$\|L(v)\|^2 \lesssim \sum_{E\in\mathcal{E}} \int_E h_E^{-1} |\underline{[\![v]\!]}|^2.$$

As similar estimate holds for $v \in V(h)$ since for $v \in H_0^1(\Omega)$, $\underline{[\![v]\!]} = 0$ and then $L(v) = 0$.

A similar argument is used for the estimation of $\|M(v)\|^2$. ∎

With these lifting operators, we introduce the perturbed forms

$$\tilde{a}_h(u, v) := \nu \int_\Omega \nabla_h u : \nabla_h v - \nu \int_\Omega (L(u) : \nabla_h v + L(v) : \nabla_h u)$$

$$+\ \nu\gamma\sum_{E\in\mathcal{E}} h_E^{-1}\int_E \underline{[\![u]\!]} : \underline{[\![v]\!]}, \qquad \forall u,v\in V(h),$$

$$\tilde{b}_h(v,q) := -\sum_{T\in T_h}\int_T q\,\mathrm{div}\,v + \sum_{E\in\mathcal{E}}\int_\Omega M(v)q, \qquad \forall v\in V(h), q\in L^2(\Omega).$$

As $\tilde{a}_h$ (resp. $\tilde{b}_h$) coincides with a_h (resp. b_h) on $V_h\times V_h$ (resp. $V_h\times Q_h$), the discrete mixed problem (3.1) is equivalent to

$$\left.\begin{array}{lcll} \tilde{a}_h(u_h,v_h)+\tilde{b}_h(v_h,p_h) &=& (f,v_h) & \forall v_h\in V_h,\\ \tilde{b}_h(u_h,q_h) &=& 0 & \forall q_h\in Q_h. \end{array}\right\}$$

Introducing the bilinear form

$$\mathcal{A}_h((u,p);(v,q)) := \tilde{a}_h(u,v)+\tilde{b}_h(v,p)-\tilde{b}_h(u,q), \forall(u,p),(v,q)\in V(h)\times L^2(\Omega),$$

problem (3.1) is also equivalent to

$$\mathcal{A}_h((u_h,p_h);(v_h,q_h)) = (f,v_h), \forall(v_h,q_h)\in V_h\times Q_h.$$

Now on $V(h)\times L^2(\Omega)$, we introduce the (natural) discontinuous Galerkin norm

$$\|(v,q)\|_{DG}^2 := \nu\|v\|_{1,h}^2+\nu^{-1}\|q\|^2, \forall(v,q)\in V(h)\times L^2(\Omega).$$

Lemma 4.1 and Cauchy-Schwarz's inequality directly lead to the continuity of $\mathcal{A}_h$ on $V(h)\times L^2(\Omega)$:

Lemma 4.2. *For all $(u,p),(v,q)\in V(h)\times L^2(\Omega)$, one has*

$$|\mathcal{A}_h((u,p);(v,q))| \lesssim \|(u,p)\|_{DG}\|(v,q)\|_{DG}.$$

Finally we need the following stability of $\mathcal{A}_h$ on $H_0^1(\Omega)^d\times L_0^2(\Omega)$:

Lemma 4.3. *For any $(u,p)\in H_0^1(\Omega)^d\times L_0^2(\Omega)$, there exists $(v,q)\in H_0^1(\Omega)^d\times L_0^2(\Omega)$ such that*

$$\mathcal{A}_h((u,p);(v,q)) \geq \|(u,p)\|_{DG}^2 \text{ and } \|(v,q)\|_{DG}\lesssim\|(u,p)\|_{DG}.$$

Proof. The proof is exactly the one given in Lemma 4.3 of [40] since for $(u,p),(v,q)\in H_0^1(\Omega)^d\times L_0^2(\Omega)$, the bilinear form $\mathcal{A}_h$ reduces to the continuous one

$$\mathcal{A}_h((u,p);(v,q)) := \nu\int_\Omega \nabla u:\nabla v - \int_\Omega p\,\mathrm{div}\,v + \int_\Omega q\,\mathrm{div}\,u,$$

and is then independent of the mesh. ∎

B. An approximation result

On V_h we introduce the other norm

$$|||v|||_{1,h}^2 := \|\nabla_h v\|^2 + |v|_{1,h}^2,$$

where the semi-norm $|\cdot|_{1,h}$ is defined by

$$|v|_{1,h} := \left(\sum_{E\in\mathcal{E}} \int_E h_E h_{min,E}^{-2} |\underline{[\![v]\!]}|^2 \, ds \right)^{1/2}.$$

Note that the property (3.4) directly implies that

$$\|v\|_{1,h} \lesssim |||v|||_{1,h}, \forall v \in V_h. \tag{4.2}$$

Consequently the norm $|||\cdot|||_{1,h}$ is stronger than the norm $\|\cdot\|_{1,h}$. For a isotropic mesh, the converse inequality holds with a constant independent of the mesh size, while it is not the case for anisotropic meshes.

Now we denote by $V_h^c = V_h \cap H_0^1(\Omega)^d$, the space of continuous element of V_h and set $V_h^\perp$ the orthogonal complement of V_h^c in V_h with respect to the inner product corresponding to the norm $|||\cdot|||_{1,h}$. The reason of this choice will be justified at the end of the section.

Theorem 4.4. *For all $v_h \in V_h^\perp$, one has*

$$|||v_h|||_{1,h} \lesssim |v_h|_{1,h} \leq |||v_h|||_{1,h}.$$

In other words the semi-norm $|\cdot|_{1,h}$ is a norm on $V_h^\perp$ equivalent to the new norm $|||\cdot|||_{1,h}$ (with constant of equivalence independent of the mesh size).

To prove the above equivalence, we follow the line of section 2.1 of [26] (see also Appendix A of [40]).

Lemma 4.5. *For all $v_h \in V_h$ and any $T \in T_h$, it holds*

$$\|\nabla v_h\|_T \lesssim |T|^{1/2} h_{min,T}^{-1} \left(\sum_{x\in\mathcal{N}_T} |v_{h|T}(x)|^2 \right)^{1/2}. \tag{4.3}$$

Proof. By a scaling argument we may write

$$\|\nabla v_h\|_T = |T|^{1/2} \|B_T^{-\top} \hat{\nabla} \hat{v}_h\|_{\hat{T}},$$

where B_T is the matrix of the affine transformation F_T that maps $\hat{T}$ to T. Since $\|B_T^{-\top}\| \lesssim h_{min,T}^{-1}$ (see [6]), we may write

$$\|\nabla v_h\|_T \lesssim |T|^{1/2} h_{min,T}^{-1} \|\hat{\nabla} \hat{v}_h\|_{\hat{T}}.$$

As all norms are equivalent on any finite-dimensional space, we conclude that

$$\|\nabla v_h\|_T \lesssim |T|^{1/2} h_{min,T}^{-1} \left(\sum_{\hat{x}\in\mathcal{N}_{\hat{T}}} |\hat{v}_h(\hat{x})|^2 \right)^{1/2}.$$

The conclusion directly follows. ∎

Lemma 4.6. *Let $v_h \in V_h$ and $E \in \mathcal{E}$. Then we have*

$$\|\underline{[\![v_h]\!]}\|_E \sim |E|^{1/2} \left(\sum_{x\in\mathcal{N}\cap E} |\underline{[\![v_h]\!]}(x)|^2 \right)^{1/2} \tag{4.4}$$

Proof. Set $w := \underline{[\![v_h]\!]}$ (which belongs to the finite-dimensional space $(\mathbb{P}^k(E))^d$ or $(\mathbb{Q}^k(E))^d$ according to the context), by a scaling argument we have

$$\| [\![v_h]\!] \|_E \sim |E|^{1/2} \|\hat{w}\|_{\hat{E}}.$$

Since $\hat{w}$ belongs to a finite-dimensional space and is uniquely determined by the nodal values at $\hat{\mathcal{N}}_T \cap \hat{E}$, we conclude as before by finite dimensionality. ∎

Lemma 4.7. *For all $v_h \in V_h$ we have*

$$\inf_{w_h \in V_h^c} \|\nabla_h (v_h - w_h)\| \lesssim |v_h|_{1,h}. \tag{4.5}$$

Proof. Assume first that the mesh is conforming. Following Theorem 2.2 of [26] (see also Lemma A.3 of [40]) we take

$$w_h = \sum_{x \in \mathcal{N}(\Omega)} \bar{v}_x \lambda_x,$$

where the nodal values of w_h are given by

$$\bar{v}_x = \frac{1}{N_x} \sum_{T \in T_h : x \in T} v_{h|T}(x),$$

where $N_x = \sum_{T \in T_h : x \in T} 1$ is the number of elements of T_h having x has node. By Lemma 4.5 for any $T \in T_h$ we have

$$\|\nabla (v_h - w_h)\|_T^2 \lesssim |T| h_{min,T}^{-2} \sum_{x \in \mathcal{N}_T} |v_{h|T}(x) - \bar{v}_x|^2.$$

Now for an internal node x by the definition of $\bar{v}_x$ and the use of discrete-Cauchy-Schwarz's inequality we get

$$\begin{aligned} |v_{h|T}(x) - \bar{v}_x|^2 &\leq \frac{1}{N_x} \sum_{T' \in T_h : x \in T'} |v_{h|T}(x) - v_{h|T'}(x)|^2 \\ &\leq \sum_{T' \in T_h : x \in T'} |v_{h|T}(x) - v_{h|T'}(x)|^2. \end{aligned}$$

This estimate in the above one yields

$$\begin{aligned} \|\nabla_h (v_h - w_h)\|^2 &\lesssim \sum_{T \in T_h} |T| h_{min,T}^{-2} \{ \sum_{x \in \mathcal{N}_T} \sum_{T' \in T_h : x \in T'} |v_{h|T}(x) - v_{h|T'}(x)|^2 \\ &+ \sum_{x \in \mathcal{N}_T \cap \partial\Omega} |v_{h|T}(x)|^2 \}. \end{aligned}$$

Using the mesh assumptions, we get

$$\begin{aligned} \|\nabla_h (v_h - w_h)\|^2 &\lesssim \sum_{E \in \mathcal{E}} h_E |E| h_{min,E}^{-2} \{ \sum_{T, T' \in T_h : E = T \cap T'} \sum_{x \in \mathcal{N}(\Omega) \cap E} |v_{h|T}(x) - v_{h|T'}(x)|^2 \\ &+ \sum_{T \in T_h : E \subset T} \sum_{x \in \mathcal{N} \cap E \cap \partial\Omega} |v_{h|T}(x)|^2 \} \\ &= \sum_{E \in \mathcal{E}} h_E |E| h_{min,E}^{-2} \sum_{x \in \mathcal{N} \cap E} |\underline{[\![v_h]\!]}(x)|^2. \end{aligned}$$

The conclusion follows by Lemma 4.6.

If T_h is nonconforming, we simply follow the proof of Theorem 2.3 of [26], taking into account the mesh assumptions and using the two above Lemmas. ∎

Theorem 4.4 directly follows from this Lemma, since the estimate (4.5) directly implies that

$$\inf_{w_h \in V_h^c} |||v_h - w_h|||_{1,h} \lesssim |v_h|_{1,h}, \forall v_h \in V_h.$$

In particular for $v_h \in V_h^\perp$, this estimate reduces to

$$|||v_h|||_{1,h} = \inf_{w_h \in V_h^c} |||v_h - w_h|||_{1,h} \lesssim |v_h|_{1,h}.$$

Let us show that this estimate (4.5) is optimal in the sense that the inverse estimate holds in some particular cases and therefore the factor $h_E h_{min,E}^{-2}$ in $|v_h|_{1,h}$ cannot be chosen smaller (for instance the factor h_E^{-1} is not convenient, see below). For that purpose take the unit square $\Omega = (-1,1)^2$ subdivided by the anisotropic mesh T_h described in Figure 1 obtained in the following way: subdivide the x_1 interval into 2 intervals $[-1,0]$ and $[0,1]$ and the x_2 interval into $2n$ uniform intervals $[y_i, y_{i+1}]$, $i = -n, \cdots, n-1$ with $y_i = ih$, $h = \frac{1}{n}$.

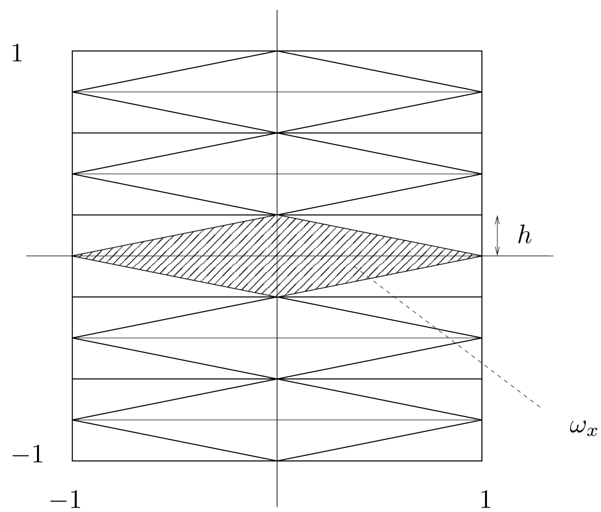

FIG. 1. The anisotropic mesh on the unit square for $n = 5$.

This yields a rectangular subdivision of Ω made of anisotropic rectangles. Subdividing each rectangle into two triangles, we get the desired anisotropic triangulation, which is conforming and satisfies our mesh assumptions. Consider the space V_h based on the triangulation T_h in the case $k = 1$. Denote by x the node of the triangulation situated at the origin. Now we fix v_h in V_h with a support on the patch ω_x, in the form

$$v_{h|T} = (v_T, 0)^\top \lambda_x, \forall T \subset \omega_x,$$

with some constants v_T, where λ_x is the standard hat function associated with x. Since the first component v_{h1} of v_h is zero outside ω_x and is continuous in $\overline{\Omega \setminus \omega_x}$, we clearly have

$$\inf_{w_h\in V_h^c} \|\nabla_h(v_h - w_h)\| = \inf_{\alpha\in\mathbb{R}} \|\nabla_h(v_{h1} - \alpha\lambda_x)\|.$$

Now in view of the form of v_{h1} we may write

$$\inf_{\alpha\in\mathbb{R}} \|\nabla_h(v_h - \alpha\lambda_x)\|^2 = \inf_{\alpha\in\mathbb{R}} \sum_{T\subset\omega_x} (v_T - \alpha)^2 \|\nabla\lambda_x\|_T^2,$$

and a direct calculation gives

$$\alpha = \frac{\sum_{T\subset\omega_x} v_T \|\nabla\lambda_x\|_T^2}{\sum_{T\subset\omega_x} \|\nabla\lambda_x\|_T^2}.$$

We further readily check that

$$\|\nabla\lambda_x\|_T^2 = h(1 + h^{-2}), \forall T \subset \omega_x,$$

and therefore

$$\alpha = \frac{1}{4} \sum_{T\subset\omega_x} v_T.$$

At this stage we take $v_T = v$ if T is included in the half-plane $x_1 \geq 0$ and $v_T = v'$ if T is included in the half-plane $x_1 \leq 0$. With this choice, we have

$$\alpha = \frac{v + v'}{2},$$

and consequently

$$\inf_{\alpha\in\mathbb{R}} \|\nabla_h(v_h - \alpha\lambda_x)\|^2 = (v - v')^2 h(1 + h^{-2}). \tag{4.6}$$

On the other hand for the above choice we have

$$|v_h|_{1,h}^2 = \sum_{i=1,2} h_{E_i} h_{min,E_i}^{-2} (v - v')^2 \int_{E_i} \lambda_x^2,$$

where E_1 and E_2 are the two edges of $\mathcal{E}$ having x as node and included in the x_2-axis (see Figure 1). As $h_{E_i} = 1$ and $h_{min,E_i} = h$, we get

$$|v_h|_{1,h}^2 = \frac{2}{3} h^{-1} (v - v')^2.$$

This identity and (4.6) show that in that case we have

$$\inf_{w_h\in V_h^c} \|\nabla_h(v_h - w_h)\| \sim |v_h|_{1,h},$$

and therefore the estimate (4.5) is optimal.

Remark that for the above choice we have

$$\sum_{E\in\mathcal{E}} \int_E h_E^{-1} |[\![v_h]\!]|^2 = \frac{2}{3}(v - v')^2 h,$$

and therefore the estimate

$$\inf_{w_h\in V_h^c} \|\nabla_h(v_h - w_h)\|^2 \lesssim \sum_{E\in\mathcal{E}} \int_E h_E^{-1} |[\![v_h]\!]|^2$$

is not true.

C. Bubble functions, extension operator, and inverse inequalities

The proof of our lower bound requires the use of some bubble functions and extension operators that satisfy certain properties.

We start with the standard case of a conforming mesh. We need two types of bubble functions, namely b_T and b_E associated with an element T and an edge/face E, respectively. For a triangle or a tetrahedron T, denoting by $\lambda_{a_i^T}$, $i = 1, \cdots, d{+}1$, the barycentric coordinates of T and by $a_i^{E,T}$, $i = 1, \cdots, d$ the vertices of the edge/face $E \subset \partial T$ we recall that

$$b_T = (d+1)^{d+1} \prod_{i=1}^{d+1} \lambda_{a_i^T} \text{ and } b_{E,T} = d^d \prod_{i=1}^{d} \lambda_{a_i^{E,T}}.$$

Similarly for a rectangle/hexahedron T and an edge/face E of T, b_T is the unique element in $\mathbb{Q}^2(T)$ such that

$$b_T = 0 \text{ on } \partial T,$$

and equal to 1 at the center of gravity of T; while the function $b_{E,T}$ is the unique element in $\mathbb{Q}^2(T)$ such that

$$b_{E,T} = 0 \text{ on } \partial T \setminus E,$$

and is equal to 1 at the center of gravity of E.

The edge/face bubble function b_E is defined on ω_E by

$$b_{E|T} = b_{E,T} \text{ on } T \subset \omega_E.$$

One recalls that

$$b_T = 0 \text{ on } \partial T, \qquad b_E = 0 \text{ on } \partial\omega_E, \qquad \|b_T\|_{\infty,T} = \|b_E\|_{\infty,\omega_E} = 1.$$

In 2D for the edge $\hat{E} \subset \partial\hat{T}$ included into the $\hat{x}$-axis, then the extension $\mathrm{F}_{\mathrm{ext}}(\hat{v}_{\hat{E}})$ of $\hat{v}_{\hat{E}} \in C(\hat{E})$ to $\hat{T}$ is defined by $\mathrm{F}_{\mathrm{ext}}(\hat{v}_{\hat{E}})(\hat{x}, \hat{y}) = \hat{v}_{\hat{E}}(\hat{x})$. For an edge $E \subset \partial T$, using the affine transformation F_T mapping $\hat{T}$ to T and $\hat{E}$ to E, $\mathrm{F}_{\mathrm{ext}}(v_E)(x, y) = \mathrm{F}_{\mathrm{ext}}(\hat{v}_{\hat{E}})(\hat{x}, \hat{y})$. We proceed similarly in 3D.

Now we may recall the so-called inverse inequalities that are proved using classical scaling techniques (cf. [36] for the isotropic case and [6] for the anisotropic case).

Lemma 4.8 Inverse inequalities. *Assume that T_h is conforming. Let $T \in T_h$ and E an edge/face of T. Let $v_T \in \mathbb{P}^{k_0}(T)$ and $v_E \in \mathbb{P}^{k_1}(E)$, for some nonnegative integers k_0 and k_1. Then the following inequalities hold, the inequality constants depending on the polynomial degree k_0 or k_1 but not on T, E or v_T, v_E.*

$$\|v_T b_T^{1/2}\|_T \sim \|v_T\|_T, \tag{4.7}$$
$$\|\nabla(v_T b_T)\|_T \lesssim h_{min,T}^{-1} \|v_T\|_T, \tag{4.8}$$
$$\|v_E b_E^{1/2}\|_E \sim \|v_E\|_E, \tag{4.9}$$
$$\|\mathrm{F}_{\mathrm{ext}}(v_E) b_E\|_T \lesssim h_{E,T}^{1/2} \|v_E\|_E, \tag{4.10}$$
$$\|\nabla(\mathrm{F}_{\mathrm{ext}}(v_E) b_E)\|_T \lesssim h_{E,T}^{1/2} h_{min,T}^{-1} \|v_E\|_E. \tag{4.11}$$

In the nonconforming case, the element bubble functions are defined in the same manner. On the contrary, edge/face bubble functions have to be modified for the hanging edges/faces. More precisely, assume that $E' \in \mathcal{E}_{hanging}$ is such that $E' \subset T \in T_h$ but is not a full edge/face of T. Then we introduce an artificial element T' such that $T' \subset T$, E' is a full edge/face of T' and that satisfies

$$|T'| \sim |T|, \tag{4.12}$$
$$h_{min,T} \lesssim h_{min,T'}. \tag{4.13}$$

Indeed if T is a triangle/tetrahedron, then T' is the triangle/tetrahedron obtained by joining E' to the vertex of T opposite to the edge/face E of T containing E' (see Figure 2). If T is a rectangle/hexahedron, then T' is the rectangle/hexahedron defined by $T' = E' \times I$, when $T = E \times I$, E being the edge/face E of T containing E' (see Figure 3).

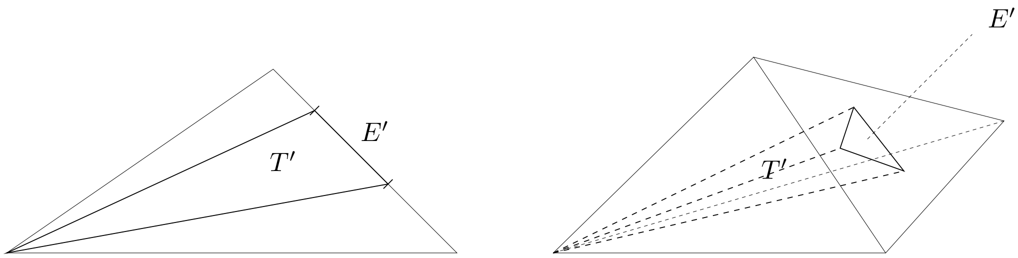

FIG. 2. Definition of T' for a triangle T (left) and a tetrahedron T (right).

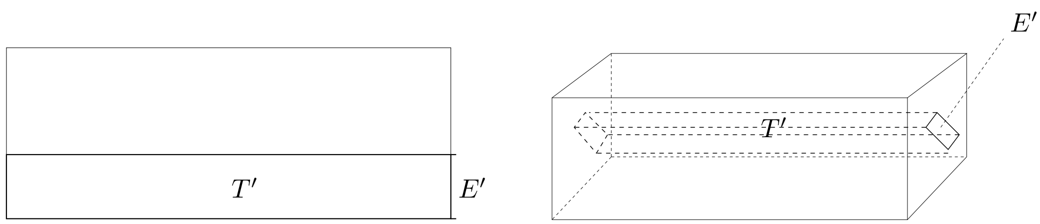

FIG. 3. Definition of T' for a rectangle T (left) and a hexahedron T (right).

Recalling that the third mesh assumption means that $|E'| \sim |E|$, we directly get the property (4.12) since

$$|T'| = |E'|h_{E',T'} = |E'|h_{E,T} \sim |E|h_{E,T} = |T|.$$

On one hand, Lemma 3.1 of [30] shows that

$$h_{min,T} \sim \rho(T),$$

where we recall that $\rho(T)$ is the diameter of the largest inscribed sphere of T. On the other hand, it is well known that

$$\rho(T) \sim \frac{|T|}{|\partial T|}.$$

Consequently the second property (4.13) holds if one can show that

$$|\partial T'| \lesssim |\partial T|.$$

If T is a rectangle or a hexahedron, this estimate is direct since $|E'| \leq |E|$ (with the above notation). For a triangle or a tetrahedron, this estimate follows from the triangular inequality.

With the help of this artificial element, we define $b_{E',T}$ as follows:

$$b_{E',T} = \begin{cases} b_{E',T'} \text{ on } T', \\ 0 \text{ on } T \setminus T'. \end{cases}$$

We finally define b_E on ω_E as before. Remark that the builded function b_E belongs to $H_0^1(\omega_E)$. Moreover the next inverse inequalities hold.

Lemma 4.9 Inverse inequalities. *If T_h is nonconforming, then the assertions of Lemma 4.8 are valid for any element $T \in T_h$ and $E \in \mathcal{E} \cap T$.*

Proof. We only need to reconsider the estimates (4.10) and (4.11) in the case when $E' \in \mathcal{E}$ is such that $E' \subset T \in T_h$ but is not a full edge/face of T. In that case, using the above notation, we first apply the inverse inequalities (4.10) and (4.11) in T', which can be written

$$\begin{aligned} \|\mathrm{F}_{\mathrm{ext}}(v_{E'})b_{E'}\|_{T'} &\lesssim h_{E',T'}^{1/2}\|v_{E'}\|_{E'}, \\ \|\nabla(\mathrm{F}_{\mathrm{ext}}(v_{E'})b_{E'})\|_{T'} &\lesssim h_{E',T'}^{1/2} h_{min,T'}^{-1}\|v_{E'}\|_{E'}. \end{aligned}$$

The requested estimates directly follow by using the properties $h_{E',T'} = h_{E',T}$, (4.13) and the fact that $b_{E'} = 0$ on $T \setminus T'$. ■

D. Anisotropic interpolation error estimates

In order to obtain an accurate discrete solution u_h, it is obvious to align the elements of the mesh according to the anisotropy of the solution. It turns out that this intuitive alignment is also necessary to prove sharp upper error bounds. In particular the proof employs specific interpolation error estimates. However, these interpolation estimates do not hold for general meshes; instead the mesh has to have the aforementioned anisotropic alignment with the function to be interpolated.

In order to quantify this alignment, we introduce a so-called alignment measure $m_1(v, T_h)$ which was originaly introduced in [29].

Definition. *[Alignment measure] Let $v \in H^1(\Omega)^d$ be a vector valued function, and T_h be a triangulation. The* alignment measure $m_1(\cdot,\cdot)$ *is then defined by*

$$m_1(v, T_h) := \frac{\left(\sum_{T \in T_h} h_{min,T}^{-2}\|\nabla v \cdot C_T\|_T^2\right)^{1/2}}{\|\nabla v\|}. \tag{4.14}$$

By definition one has $m_1(v, T_h) \geq 1$. For arbitrary isotropic meshes one obtains that $m_1(v, T_h) \sim 1$. The same is achieved for anisotropic meshes T_h that are aligned with the anisotropic function v. Therefore the alignment measure is not an obstacle for reliable error estimation.

Since the focus of our work is on a posteriori error estimation, we refer to [41, 29] for some discussions on this alignment measure.

Contrary to the (standard) Galerkin method where the interpolant has to be continuous, here we do not need its continuity since our interpolant only needs to belong to V_h. Therefore the projection on piecewise constant function is sufficient. For $v \in L^2(\Omega)$, we recall that this projection $\mathcal{M}_h v$ is given by

$$(\mathcal{M}_h v)_{|T} = \mathcal{M}_T v, \forall T \in T_h.$$

For a vector-valued function v, we define its projection $\mathcal{M}_h v$ componentwise.

Lemma 4.10 Local interpolation error bounds. *Let $v \in H_0^1(\Omega)$. Then*

$$\|v - \mathcal{M}_T v\|_T \lesssim \|C_T^\top \nabla v\|_T, \qquad \forall T \in T_h, \tag{4.15}$$

$$h_E \|v - \mathcal{M}_T v\|_E^2 \lesssim \|C_T^\top \nabla v\|_T^2, \qquad \forall T \in T_h, E \in \mathcal{E} \cap T. \tag{4.16}$$

Proof. The first inequality (4.15) has been proven in [29, Lemma 4]. The same scaling argument and the compact embedding of $H^1(\hat{T})$ into $L^2(\hat{E})$ yield the second estimate. ∎

Lemma 4.11 Global interpolation error bounds. *Let $v \in H_0^1(\Omega)^d$. Then*

$$\sum_{T \in T_h} h_{min,T}^{-2} \|v - \mathcal{M}_T v\|_T^2 \lesssim m_1(v, T_h)^2 \|\nabla v\|^2, \tag{4.17}$$

$$\sum_{E \in \mathcal{E}} h_E h_{min,E}^{-2} \| \{\{v - \mathcal{M}_h v\}\} \|_E^2 \lesssim m_1(v, T_h)^2 \|\nabla v\|^2. \tag{4.18}$$

Proof. Direct consequence of the previous lemma and the definition of the alignment measure. ∎

V. ERROR ESTIMATES

Here we present our main results, namely reliable and efficient error estimation on *anisotropic meshes*. Our main contributions are the anisotropic character of the error estimates, the proof of the upper error bound with our mesh assumptions and the proof of the lower bound.

A. Residual error estimators

The exact residuals are defined by

$$R_T := f - (-\nu \Delta u_h + \nabla p_h) \text{ on } T.$$

Define the gradient jump in normal direction by

$$J_{E,n} := \begin{cases} [\![\nu \nabla_h u_h - p_h \mathrm{I}]\!] & \text{for } E \in \mathcal{E} \text{ such that } E \subset \Omega, \\ 0 & \text{for boundary edges/faces } E. \end{cases}$$

Definition. *[Residual error estimator] The local and global residual error estimators are defined by*

$$\begin{aligned} \eta_T^2 &:= h_{min,T}^2 \nu^{-1} \|R_T\|_T^2 + \nu \|\operatorname{div} u_h\|_T^2 \\ &+ \sum_{E \in \mathcal{E}: E \subset \partial T} \left(h_{min,T}^2 h_E^{-1} \nu^{-1} \|J_{E,n}\|_E^2 + \nu h_E h_{min,E}^{-2} \| \underline{[\![u_h]\!]} \|_E^2 \right), \\ \eta^2 &:= \sum_{T \in T_h} \eta_T^2. \end{aligned}$$

B. Proof of the upper error bound

We proceed as [27] with the necessary adaptations due to the anisotropy of the mesh.

According to the results from the previous section, we define the following modified discontinuous Galerkin norm on $V(h) \times L^2(\Omega)$

$$\|(v,q)\|_{DGM}^2 := \nu |||v|||_{1,h}^2 + \nu^{-1}\|q\|^2 = \nu\|\nabla_h v\|^2 + \nu |v|_{1,h}^2 + \nu^{-1}\|q\|^2.$$

Note that

$$\|(v,q)\|_{DG} \lesssim \|(v,q)\|_{DGM}, \forall (v,q) \in V(h) \times L^2(\Omega),$$

and that

$$\|(v,q)\|_{DG} = \|(v,q)\|_{DGM}, \forall (v,q) \in H_0^1(\Omega) \times L^2(\Omega).$$

We start with the following estimate:

Lemma 5.1. *Let $(v,q) \in H_0^1(\Omega)^d \times L_0^2(\Omega)$, then we have*

$$|(f, v - \mathcal{M}_h v) - \mathcal{A}_h((u_h,p_h);(v - \mathcal{M}_h v, q))| \lesssim m_1(v, T_h)\eta\|(v,q)\|_{DG}.$$

Proof. Elementwise integrations by parts lead to

$$\begin{aligned}
&(f, v - \mathcal{M}_h v) - \mathcal{A}_h((u_h,p_h);(v - \mathcal{M}_h v, q)) \\
&= \sum_{T\in T_h} \Big(\int_T R_T \cdot (v - \mathcal{M}_h v) - \int_T q \operatorname{div} u_h\Big) \\
&+ \sum_{E\in\mathcal{E}} \int_E J_{E,n} \cdot \{\{v - \mathcal{M}_h v\}\} - \nu\gamma \sum_{E\in\mathcal{E}} h_E^{-1} \int_E \underline{[\![u_h]\!]} : \underline{[\![v - \mathcal{M}_h v]\!]} \\
&+ \nu \int_\Omega L(u_h) : \nabla_h (v - \mathcal{M}_h v) + \int_\Omega M(u_h) q.
\end{aligned}$$

Applying Cauchy-Schwarz's inequality we obtain

$$\begin{aligned}
&|(f, v - \mathcal{M}_h v) - \mathcal{A}_h((u_h,p_h);(v - \mathcal{M}_h v, q)| \le \left(\sum_{T\in T_h} \|\operatorname{div} u_h\|_T^2\right)^{1/2} \|q\| \\
&+ \left(\sum_{T\in T_h} h_{min,T}^2 \|R_T\|_T^2\right)^{1/2} \left(\sum_{T\in T_h} h_{min,T}^{-2} \|v - \mathcal{M}_h v\|_T^2\right)^{1/2} \\
&+ \left(\sum_{E\in\mathcal{E}} h_{min,E}^2 h_E^{-1} \|J_{E,n}\|_E^2\right)^{1/2} \left(\sum_{E\in\mathcal{E}} h_{min,E}^{-2} h_E \|\{\{v - \mathcal{M}_h v\}\}\|_E^2\right)^{1/2} \\
&+ \nu \left(\sum_{E\in\mathcal{E}} h_E^{-3} h_{min,E}^2 \|\underline{[\![u_h]\!]}\|_E^2\right)^{1/2} \left(\sum_{E\in\mathcal{E}} h_E h_{min,E}^{-2} \|\underline{[\![v - \mathcal{M}_h v]\!]}\|_E^2\right)^{1/2} \\
&+ \nu \left(\sum_{T\in T_h} h_{min,T}^2 \|L(u_h) C_T^{-T}\|_T^2\right)^{1/2} \left(\sum_{T\in T_h} h_{min,T}^{-2} \|\nabla_h (v - \mathcal{M}_h v) C_T\|_T^2\right)^{1/2} \\
&+ \|M(u_h)\|\|q\|.
\end{aligned}$$

We conclude by the estimate (3.4) and Lemmas 4.1 and 4.11 since $\|C_T^{-T}\|_2 = h_{min,T}^{-1}$ [6]. ∎

With the help of this Lemma we can obtain the requested upper error bound for our anisotropic DG discretization.

Theorem 5.2. *Let $(u,p) \in H_0^1(\Omega)^d \times L_0^2(\Omega)$ be the unique solution of (2.2) and $(u_h, p_h) \in V_h \times Q_h$ be the unique solution of (3.1). Denote by $u_h^c \in V_h^c$ the orthogonal projection of u_h on V_h^c corresponding to the orthogonal decomposition of V_h introduced in section B.. Let $(v,q) \in H_0^1(\Omega)^d \times L_0^2(\Omega)$ be the pair obtained in Lemma 4.3 corresponding to $(u - u_h^c, p - p_h)$. Then the error is bounded globally from above by*

$$\|(u-u_h, p-p_h)\|_{DG} \lesssim \|(u-u_h, p-p_h)\|_{DGM} \lesssim\ m_1(v, T_h)\eta. \tag{5.1}$$

Proof. Following subsection 4.4 of [27], we first write $u_h = u_h^c + u_h^\perp$, with $u_h^c \in V_h^c$ and $u_h^\perp \in V_h^\perp$, corresponding to the orthogonal decomposition of V_h introduced in section B.. Consequently we may write

$$\|(u-u_h, p-p_h)\|_{DGM}^2 \le 2\|(u-u_h^c, p-p_h)\|_{DGM}^2 + 2\nu|||u_h^\perp|||_{1,h}^2,$$

and by Theorem 4.4, we deduce that

$$\|(u-u_h, p-p_h)\|_{DGM}^2 \lesssim \|(u-u_h^c, p-p_h)\|_{DGM}^2 + \nu|u_h^\perp|_{1,h}^2.$$

As $\underline{[\![u_h^\perp]\!]} = \underline{[\![u_h]\!]}$, in view of the definition of η, we arrive at

$$\|(u-u_h, p-p_h)\|_{DGM}^2 \lesssim \|(u-u_h^c, p-p_h)\|_{DGM}^2 + \eta^2. \tag{5.2}$$

So it remains to estimate $\|(u-u_h^c, p-p_h)\|_{DGM}^2$, which reduces to

$$\|(u-u_h^c, p-p_h)\|_{DGM}^2 = \nu\|\nabla_h(u-u_h^c)\|^2 + \nu^{-1}\|p-p_h\|^2 = \|(u-u_h^c, p-p_h)\|_{DG}^2.$$

Using Lemma 4.3 we then may write

$$\begin{aligned}\|(u-u_h^c, p-p_h)\|_{DG}^2 &\le \mathcal{A}_h((u-u_h^c, p-p_h);(v,q)) \\ &= \mathcal{A}_h((u-u_h, p-p_h);(v,q)) + \mathcal{A}_h((u_h^\perp, 0);(v,q)).\end{aligned}$$

Using (2.2) and (3.1), we arrive at

$$\begin{aligned}\|(u-u_h^c, p-p_h)\|_{DG}^2 &\le (f, v-\mathcal{M}_h v) - \mathcal{A}_h((u_h, p_h);(v-\mathcal{M}_h v, q)) \\ &+\ \mathcal{A}_h((u_h^\perp, 0);(v,q)).\end{aligned}$$

Lemmas 4.2 and 5.1 lead to

$$\|(u-u_h^c, p-p_h)\|_{DG}^2 \lesssim (m_1(v,T_h)\eta + \|u_h^\perp\|_{1,h})\|(v,q)\|_{DG}.$$

By the estimate (4.2), and arguments already used above, we have

$$\|u_h^\perp\|_{1,h} \lesssim \eta.$$

These two estimates and the bound $\|(v,q)\|_{DG} \lesssim \|(u-u_h^c, p-p_h)\|_{DG}$ from Lemma 4.3 lead to

$$\|(u-u_h^c, p-p_h)\|_{DGM} = \|(u-u_h^c, p-p_h)\|_{DG} \lesssim m_1(v,T_h)\eta. \tag{5.3}$$

The conclusion follows from the two estimates (5.2) and (5.3). ∎

C. Proof of the lower error bound

Theorem 5.3 Lower error bound. *For all elements T, the following local lower error bound holds:*

$$\eta_T^2 \lesssim \nu\|\nabla_h(u-u_h)\|_{\omega_T}^2 + \nu^{-1}\|p-p_h\|_{\omega_T}^2 + \nu \sum_{E\in\mathcal{E}:E\subset T} h_E h_{min,E}^{-2} \|\underline{[\![u-u_h]\!]}\|_E^2. \quad (5.4)$$

Proof. The estimate

$$\begin{aligned} h_{min,T}^2\nu^{-1}\|R_T\|_T^2 + \nu\|\mathrm{div}\, u_h\|_T^2 \ &+ \ \nu^{-1}\sum_{E\in\mathcal{E}:E\subset T} \frac{h_{min,T}^2}{h_E}\|J_{E,n}\|_E^2 \\ \lesssim \nu\|\nabla_h(u-u_h)\|_{\omega_T}^2 \ &+ \ \nu^{-1}\|p-p_h\|_{\omega_T}^2 \end{aligned} \quad (5.5)$$

was proved in Theorem 6.2 of [22] for $\nu = 1$ and a conforming mesh using bubble functions, integration by parts and the inverse inequalities from Lemma 4.8. The proof is similar when $\nu \neq 1$ and in the nonconforming case using the new edge/face bubble functions introduced in section C. and the inverse inequalities from Lemma 4.9. We give it for the sake of completeness.

We bound each of the residuals separately.

Element residual: Set $w_T := R_T b_T \in H_0^1(T)^d$ and integrate by parts to obtain

$$\begin{aligned} \int_T R_T\cdot w_T \ &= \ \int_T (-\nu\Delta(u-u_h) + \nabla(p-p_h))\cdot w_T \\ &= \ \nu\int_T (\nabla(u-u_h) - (p-p_h)\mathrm{I}) : \nabla w_T \\ &\le \ (\nu\|\nabla(u-u_h)\|_T + \|p-p_h\|_T)\,\|\nabla w_T\|_T. \end{aligned}$$

The inverse inequalities (4.7) and (4.8) imply

$$\|R_T\|_T \ \lesssim \ h_{min,T}^{-1}(\nu\|\nabla(u-u_h)\|_T + \|p-p_h\|_T). \quad (5.6)$$

Divergence: Since u is divergence free, one directly concludes

$$\|\mathrm{div}\, u_h\|_T = \|\mathrm{div}\,(u-u_h)\|_T \le \sqrt{d}\,\|\nabla(u-u_h)\|_T. \quad (5.7)$$

Normal jump: For $E\in\mathcal{E}$ such that $E\subset\Omega$, we may write $\omega_E = T_1\cup T_2$ and assume that $T\equiv T_1$. Recall that $J_{E,n}\in\mathbb{P}^l(E)^d$ for some $l\in\mathbb{N}$ depending on the chosen finite element space. Set

$$w_E := \mathrm{F}_{\mathrm{ext}}(J_{E,n})b_E \in H_0^1(\omega_E)^d.$$

Partial integration on ω_E yields

$$\int_{\omega_E} f\cdot w_E = \int_{\omega_E} (-\nu\Delta u + \nabla p)\cdot w_E \ = \ \int_{\omega_E} (\nu\nabla u - p\mathrm{I}) : \nabla w_E.$$

By elementwise partial integration we further conclude (recalling that if E is not equal to $T_1\cap T_2$, then $b_{E|T_1\cap T_2}$ is equal to zero outside E)

$$-\int_E J_{E,n}\cdot w_E \ = \ \sum_{i=1}^2 \int_{\partial T_i} (\nu\nabla u_h - p_h\mathrm{I})n\cdot w_E$$

$$= \int_{\omega_E} (\nu \nabla u_h - p_h \mathrm{I}) : \nabla w_E \; - \; \sum_{i=1}^{2} \int_{T_i} (-\nu \Delta u_h + \nabla p_h) \cdot w_E.$$

The above identity and Cauchy-Schwarz's inequality then imply

$$\begin{aligned} \int_E J_{E,n} \cdot w_E \; &= \; \int_{\omega_E} (\nu \nabla (u - u_h) - (p - p_h)\mathrm{I}) : \nabla w_E \\ &- \; \sum_{i=1}^{2} \int_{T_i} (f - (-\nu \Delta u_h + \nabla p_h)) \cdot w_E \\ &\leq \; (\nu \| \nabla_h (u - u_h) \|_{\omega_E} + \| p - p_h \|_{\omega_E}) \, \| \nabla w_E \|_{\omega_E} \\ &+ \; \sum_{i=1}^{2} \| R_{T_i} \|_{T_i} \| w_E \|_{T_i}. \end{aligned}$$

The inverse inequalities (4.9)–(4.11) from Lemma 4.8 or 4.9 and the previous bound (5.6) of $\|R_{T_i}\|_{T_i}$ imply

$$\frac{h^2_{min,T}}{h_E} \| J_{E,n} \|^2_E \; \lesssim \; \nu^2 \| \nabla_h (u - u_h) \|^2_{\omega_E} + \| p - p_h \|^2_{\omega_E}. \tag{5.8}$$

For a boundary edge/face nothing needs to be done since $J_{E,n} \equiv 0$ there.

The estimate (5.5) directly follows from (5.6) to (5.8). The conclusion readily follows from this estimate (5.5) since $\underline{[\![u - u_h]\!]} = -\underline{[\![u_h]\!]}$. ∎

Corollary. *[Global lower error bound] The following global lower error bound holds:*

$$\eta \lesssim \| (u - u_h, p - p_h) \|_{DGM}. \tag{5.9}$$

Consequently if $m_1(v, T_h) \sim 1$, we have the next equivalence

$$\eta \sim \| (u - u_h, p - p_h) \|_{DGM}.$$

Remark. *[Alignment measure]* The upper error bound (5.1) contains the alignement measure $m_1(v, T_h)$ that cannot be evaluated explicitly. This is in contrast to estimators for isotropic meshes: For anisotropic discretizations, all known estimators assume explicitly or implicitly that the meshes are suitably aligned with the solution. However, this should not be considered too much as a disadvantage. Indeed, the alignment measure $m_1(u - u_h, T_h)$ for the velocity error is of size $\mathcal{O}(1)$ for sufficiently good meshes [29, 30, 42] and therefore we may expect a similar behaviour for $m_1(v, T_h)$. This confidence is strengthened by the numerical experiments below.

In practical computations one may simply use the error estimator without considering the alignment measure. For adaptive algorithms this is well justified since the lower error bound holds unconditionally, i.e. the estimator is efficient.

D. Application to isotropic discretizations

Since our analysis gives new results for isotropic meshes, we here summarize them. In that case our conclusions hold with $h_{min,T} \sim h_E \sim h_T$ for $E \subset \partial T$ (recalling that h_T is the diameter of T) and the alignment measure $m_1(v, T_h) \sim 1$. In other words, the above results may be rephrased as follows: the residual error estimator is here given by

$$\eta_T^2 := h_T^2 \nu^{-1} \| R_T \|^2_T + \nu \| \mathrm{div}\, u_h \|^2_T + \sum_{E \subset \partial T} \left(h_T \nu^{-1} \| J_{E,n} \|^2_E + \nu h_T^{-1} \| \underline{[\![u_h]\!]} \|^2_E \right).$$

With this definition, the local lower error bound (5.4) of Theorem 5.3 holds for any isotropic elements T, while the upper bound (5.1) reduces to

$$\|(u - u_h, p - p_h)\|_{DG} \lesssim \eta.$$

In particular we have the equivalence

$$\|(u - u_h, p - p_h)\|_{DG} \sim \eta,$$

which mean that the estimator is efficient and reliable.

VI. NUMERICAL EXPERIMENTS

The following experiments will underline and confirm our theoretical predictions. These comparatively simple 2D problems also serve as first tests to justify the more elaborate and voluminous 3D tests. With the limitations of the experiments in mind, we can nevertheless draw valuable conclusions.

The present numerical tests consist in solving the two dimensional Stokes problem (2.1) given in its mixed formulation (2.2) on the unit square $\Omega = (0,1)^2$ with $\nu = 1$. The approximation of the problem is ensured by a discontinuous Galerkin discretization. Each mesh is an anisotropic Shishkin type one composed of triangles, defined as the tensor product of a 1D Shishkin type mesh and a uniform mesh both with n subintervals (see Figure 4). The parameter $\tau \in (0,1)$ is a transition point parameter, defining the coordinates (x_i, y_j) of the nodes of the triangles by :

$$dx_1 := 2\tau/n, \quad dx_2 := 2(1-\tau)/n, \quad dy = 1/n,$$

$$\begin{cases} x_i := i\,dx_1 & (0 \le i \le n/2), \\ x_i := \tau + (i - n/2)\,dx_2 & (n/2+1 \le i \le n), \\ y_j := j\,dy & (0 \le j \le n). \end{cases}$$

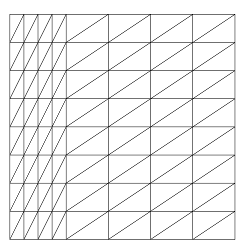

τ

FIG. 4. Shishkin type mesh on the unit square with $n = 8$ and $\tau = 0.25$.

Defining the approximation spaces V_h and Q_h as in subsection B. with $d = 2$ and $k = 1$, we are looking for $u_h \in V_h$ and $p_h \in Q_h$ satisfying the variationnal formulation (3.1). The discrete problem (3.1) is solved with the classical Uzawa algorithm, with the parameter γ equal to 100. The number of degrees of freedom is equal to $6n^2$ for each component of the velocity, and to $2n^2$ for the pressure. The total number of degrees of freedom (DoF) is then equal to $14n^2$.

A. Isotropic solution

This first test is performed with the following prescribed exact solution (u, p) :

$$\begin{cases} \Phi = x^2(1-x)^2y^2(1-y)^2, \\ u = \operatorname{curl}\Phi, \\ p = x - \frac{1}{2}. \end{cases}$$

This allows to have in particular $\operatorname{div} u = 0$, $u_{|\Gamma} = 0$, and the mean value of p on the domain equal to zero. Note that for this test, the parameter τ is taken equal to 0.5, making the mesh isotropic.

To begin with, let us check that the numerical solution (u_h, p_h) converges towards the exact one. To this end we plot the curve $||u - u_h, p - p_h||_{DG}$ as a function of DoF (see Figure 5).

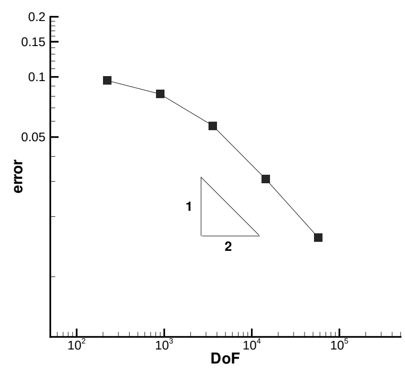

FIG. 5. $||(u - u_h, p - p_h)||_{DG}$ in dependence of DoF.

As we can see, the convergence rates is of order 0.5 in DoF, as theoretically expected. This shows the good convergence of (u_h, p_h) towards (u, p).

Now we investigate the main theoretical results which are the upper and the lower error bounds. In order to present the underlying inequalities in Theorems 5.2 and 5.3 appropriately, we reformulate them by defining the ratios of left-hand side and right-hand side, respectively:

$$q_{\text{up}} = \frac{||(u - u_h, p - p_h)||_{DG}}{\eta},$$

$$q_{\text{low}} = \max_{T \in T_h} \frac{\eta_T}{\sqrt{\nu||\nabla_h(u - u_h)||^2_{\omega_T} + \nu^{-1}||p - p_h||^2_{\omega_T} + \nu \sum_{E \subset T} h_E h^{-2}_{min,E} || \underline{[\![u - u_h]\!]} ||^2_E}}.$$

The first ratio q_{up} is frequently referred to as *effectivity index*. It measures the *reliability* of the estimator and is related to the global upper error bound. As isotropic meshes are used here, the alignment measures $m_1(v, T_h)$ from Theorem 5.2 is of size 1. Therefore, according to Theorem 5.2, the corresponding ratio q_{up} should be bounded from above. This is confirmed by the experiment (left part of Figure 6). Thus the estimator is *reliable*.

The second ratio is related to the local lower error bound and measures the *efficiency* of the estimator. According to Theorem 5.3, q_{low} has to be bounded from above. This can be observed indeed in the right part of figure 6. Hence the estimator is *efficient*.

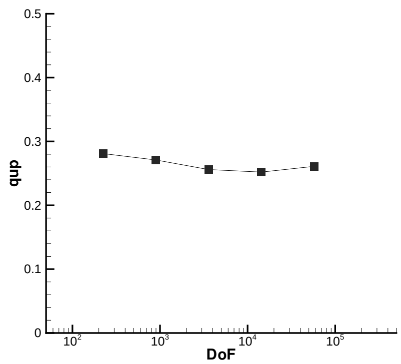

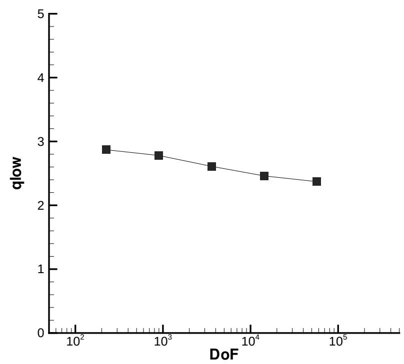

FIG. 6. q_{up} (left) and q_{low} (right) in dependence of DoF, isotropic solution.

B. Anisotropic solution

This second test is performed with the following prescribed exact solution (u, p) :

$$\begin{cases} \Phi &= x^2(1-x)^2y^2(1-y)^2e^{-x/\sqrt{\varepsilon}}, \\ u &= \operatorname{curl}\Phi, \\ p &= e^{-x/\sqrt{\varepsilon}} - \sqrt{\varepsilon}(1-e^{-\frac{1}{\sqrt{\varepsilon}}}). \end{cases}$$

As previously, we have in particular $\operatorname{div} u = 0$, $u_{|\Gamma} = 0$, and the mean value of p on the domain equal to zero. Note that u and p present an exponential boundary layer of width $\mathcal{O}(\sqrt{\epsilon})$ along the line $x = 0$. The transition parameter τ involved in the construction of the Shishkin-type mesh is defined by $\tau := \min\{1/2, 2\sqrt{\epsilon}|\ln\sqrt{\epsilon}|\}$, i.e. it is roughly twice the boundary layer width.

As before, we first check the convergence of the numerical solution (u_h, p_h) towards the exact one, by plotting the curve $||(u-u_h, p-p_h)||_{DG}$ as a function of DoF (see Figure 7).

As we can see, for each value of ε, the convergence rate is of order 0.5 in DoF, as theoretically expected. This shows the good convergence of (u_h, p_h) towards (u, p), independently of the value of ε.

Now let us investigate the upper and lower error bounds. The definitions of q_{up} and q_{low} are the same as in the previous test. As we employ well adapted meshes, we may expect that the alignment measures $m_1(v, T_h)$ is of moderate size. As soon as a reasonable resolution of the layer is achieved, the results on figure 8 show that the estimator is efficient and reliable. Moreover, the values of q_{up} and q_{low} are independant of ε, and take values similar to the ones for other problem classes [29, 30, 43, 44, 31, 32]. We further emphasize that we do not attempt to reach effectivity indices of around one but rather to show that the effectivity index does not vary too much with respect to a family of convenient meshes, which is clearly confirmed here by our test.

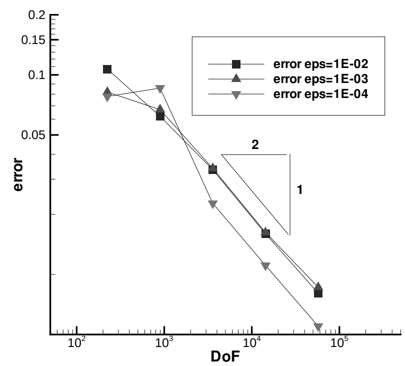

FIG. 7. $||(u - u_h, p - p_h)||_{DG}$ in dependence of DoF.

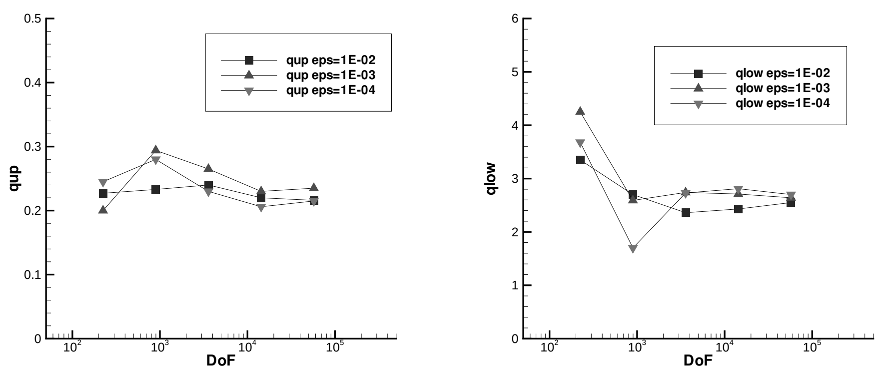

FIG. 8. q_{up} (left) and q_{low} (right) in dependence of DoF, anisotropic solution.

REFERENCES

1. H.-G. Roos, M. Stynes, and L. Tobiska. *Numerical methods for singularly perturbed differential equations. Convection-diffusion and flow problems*. Springer, Berlin, 1996.
2. T. Apel, S. Nicaise, and J. Schöberl. A non-conforming finite element method with anisotropic mesh grading for the Stokes problem in domains with edges. *IMA J. Numer. Anal.*, 21:843–856, 2001.
3. D. Schötzau and C. Schwab. Mixed *hp*-FEM on anisotropic meshes. *Math. Models Methods Appl. Sci.*, 8:787–820, 1998.
4. D. Schötzau, C. Schwab, and R. Stenberg. Mixed *hp*-FEM on anisotropic meshes II: Hanging nodes and tensor products of boundary layer meshes. *Numer. Math.*, 83:667–697, 1999.
5. A. Toselli and C. Schwab. Mixed *hp*-finite element approximations on geometric boundary layer meshes in R^3. *C.R.Acad. Paris Série I*, 332:857–862, 2001.
6. G. Kunert. *A posteriori error estimation for anisotropic tetrahedral and triangular finite element meshes*. Logos Verlag, Berlin, 1999. Also PhD thesis, TU Chemnitz, http://archiv.tu-chemnitz.de/pub/1999/0012/index.html.
7. L. Formaggia, S. Perotto, and P. Zunino. An anisotropic a-posteriori error estimate for a convection-diffusion problem. *Comput. Vis. Sci.*, 4(2):99–104, 2001.
8. M. J. Castro-Díaz, F. Hecht, and B. Mohammadi. New progress in anisotropic grid adaption for inviscid and viscous flow simulations. In *Proceedings of the* 4^{th} *Annual International Meshing Roundtable*, pages 73–85, Albuquerque, NM, 1995. Sandia National Laboratories. Also Report 2671 at INRIA.
9. B. Cockburn, G. E. Karniadakis, and C.-W. Shu. *The development of discontinuous Galerkin methods*, volume 11 of *Lect. Notes Comput. Sci. Eng.* Springer Verlag, Berlin, 2000.
10. D. G. Arnold, F. Brezzi, B. Cockburn, and L. D. Marini. Unified analysis of discontinuous Galerkin methods for elliptic problems. *SIAM J. Numer. Anal.*, 39:1749–1779, 2001.
11. G. A. Baker, W. N. Jureidini, and O. A. Karakashian. Piecewise solenoidal vector fields and the Stokes problem. *SIAM J. Numer. Anal.*, 27:1466–1485, 1990.
12. O. A. Karakashian and W. N. Jureidini. A nonconforming finite element method for the stationary Navier-Stokes equations. *SIAM J. Numer. Anal.*, 35:93–120, 1998.
13. B. Cockburn, G. Kanschat, D. Schötzau, and C. Schwab. Local discontinuous Galerkin methods for the Stokes problem. *SIAM J. Numer. Anal.*, 40:319–343, 2002.
14. A. Toselli. *hp*-Discontinuous Galerkin approximations for the Stokes problem. *Math. Models Meth. Appl. Sci.*, 12:1565–1616, 2002.
15. D. Schötzau, C. Schwab, and A. Toselli. Mixed *hp*-DGFEM for incompressible flows. *SIAM J. Numer. Anal.*, 40:2171–2194, 2003.
16. R. Verfürth. A posteriori error estimators for the Stokes equation. *Numer. Math.*, 55:309–325, 1989.
17. R. E. Bank and B. D. Welfert. A posteriori error estimates for the Stokes equations: a comparison. *Comput. Methods Appl. Mech. Engrg.*, 82:323–340, 1990.
18. E. Dari, R. Durán, and C. Padra. Error estimators for nonconforming finite element approximations of the Stokes problem. *Math. Comput.*, 64(211):1017–1033, 1995.
19. M. Ainsworth and J. Oden. A posteriori error estimators for the Stokes and Oseen equations. *SIAM J. Num. Anal.*, 34(1):228–245, 1997.
20. D. Kay and D. Silvester. A posteriori error estimation for stabilized mixed approximations of the Stokes equations. *SIAM J. Sci. Comput.*, 21(4):1321–1336, 2000.

21. C. Carstensen and S. Funken. A posteriori error control in low-order finite element discretisations of incompressible stationary flow problems. *Math. Comp.*, 70(236):1353–1381, 2001.
22. E. Creusé, G. Kunert, and S. Nicaise. A posteriori error estimation for the Stokes problem: Anisotropic and isotropic discretizations. *Math. Models Methods Appl. Sci.*, 14:1297–1341, 2004.
23. M. Picasso. An adaptive algorithm for the Stokes problem using continuous, piecewise linear stabilized finite elements and meshes with high aspect ratio. *Applied Numerical Mathematics*. to appear.
24. R. Becker, P. Hansbo, and M. G. Larson. Energy norm a posteriori error estimation for discontinuous Galerkin methods. *Comput. Meth. Appl. Mech. Engrg.*, 192:723–733, 2003.
25. R. Becker, P. Hansbo, and R. Stenberg. A finite element method for domain decomposition with non-matching grids. *Modél. Math. Anal. Numér.*, 37:209–225, 2003.
26. O. A. Karakashian and F. Pascal. A posteriori error estimates for a discontinuous Galerkin approximation of second-order problems. *SIAM J. Numer. Anal.*, 41:2374–2399, 2003.
27. P. Houston, D. Schötzau, and T. Wihler. Energy norm a posteriori error estimation for mixed discontinuous Galerkin approximations of the Stokes problem. *J. Scientific Computing*, 22(1):357–380, 2005.
28. V. Girault and P.-A. Raviart. *Finite element methods for Navier-Stokes equations, Theory and algorithms*, volume 5 of *Springer Series in Computational Mathematics*. Springer, Berlin, 1986.
29. G. Kunert. An a posteriori residual error estimator for the finite element method on anisotropic tetrahedral meshes. *Numer. Math.*, 86(3):471–490, 2000. DOI 10.1007/s002110000170.
30. G. Kunert. Robust a posteriori error estimation for a singularly perturbed reaction–diffusion equation on anisotropic tetrahedral meshes. *Adv. Comp. Math.*, 15(1–4):237–259, 2001.
31. M. Picasso. An anisotropic error indicator based on Zienkiewicz-Zhu error estimator: Application to elliptic and parabolic problems. *SIAM J. Sci. Comput.*, 24(4):1328–1355, 2003.
32. M. Picasso. Anisotropic, adaptive, stabilized finite elements for Stokes problem. *Comput. Methods Appl. Mech. Eng.*, 2003. submitted.
33. P. Houston, I. Perugia, and D. Schötzau. Energy norm a posteriori error estimation for mixed discontinuous Galerkin approximations of the Maxwell operator. *Comput. Meth. Appl. Mech. Engrg.*, 194:499–510, 2005.
34. P. Hansbo and M. G. Larson. Discontinuous finite element methods for incompressible and nearly incompressible elasticity by use of Nitsche's method. *Comput. Meth. Appl. Mech. Engrg.*, 191:1895–1908, 2002.
35. P. G. Ciarlet. *The finite element method for elliptic problems*. North-Holland, Amsterdam, 1978.
36. R. Verfürth. *A review of a posteriori error estimation and adaptive mesh–refinement techniques*. Wiley and Teubner, Chichester and Stuttgart, 1996.
37. F. Brezzi and M. Fortin. *Mixed and hybrid finite element methods*. Springer-Verlag, New York, 1991.
38. M. Dauge. *Elliptic boundary value problems on corner domains – smoothness and asymptotics of solutions*, volume 1341 of *Lecture Notes in Mathematics*. Springer, Berlin, 1988.
39. I. Perugia and D. Schötzau. An hp-analysis of the local discontinuous Galerkin method for diffusion problems. *J. Sci. Comp.*, 17:561–571, 2002.

40. P. Houston, I. Perugia, and D. Schötzau. Mixed discontinuous Galerkin approximation of the Maxwell operator. *SIAM J. Numer. Anal.*, 42:434–459, 2004.

41. G. Kunert. A local problem error estimator for anisotropic tetrahedral finite element meshes. *SIAM J. Numer. Anal.*, 39(2):668–689, 2001.

42. G. Kunert. Towards anisotropic mesh construction and error estimation in the finite element method. *Numer. Meth. PDE*, 18(6):625–648, 2002.

43. M. Picasso. Numerical study of the effectivity index for an anisotropic error indicator based on Zienkiewicz-Zhu error estimator. *Commun. Numer. Meth. Engrg*, 19(1):13–23, 2003.

44. R. Becker, P. Hansbo, and M. L. Larson. Energy norm a posteriori error estimation for discontinuous Galerkin methods. *Calcolo*, 2003. submitted.